PERGAMON

International Journal of Solids and Structures 40 (2003) 3347–3377

INTERNATIONAL JOURNAL OF SOLIDS and STRUCTURES

www.elsevier.com/locate/ijsolstr

Analysis of scattering waves in an elastic layered medium by means of the complete eigenfunction expansion form of the Green's function

Terumi Touhei

Department of Civil Engineering, Tokyo University of Science, 2641, Yamazaki Noda City 278-8510, Japan

Received 19 August 2002; received in revised form 12 February 2003

Abstract

A scattering problem due to an object and a plane incident wave in an elastic layered half space is presented in this paper. The complete eigenfunction expansion form of the Green's function developed by the author and the boundary integral equation method are introduced into the analysis. First, the complete eigenfunction expansion form of the Green's function is investigated for its application to the scattering problem. A comprehensive explanation is also given for the fact that the complex Rayleigh wave modes exhibit standing waves. Next, a method for the analysis of scattering waves by means of the Green's function is presented. The advantage of the present method is that the formulation itself is independent of the number of layers and the scattering waves can be decomposed into the modes for the spectra defined for the layered medium. Several numerical calculations are performed to examine the efficiency of the present method as well as the properties of the scattering waves. According to the numerical results, the complete eigenfunction expansion form of the Green's function provides accurate values for application to a boundary element analysis. The spectral structure and radiation patterns of the scattering wave are presented and investigated. The differences in directionality can be found from the radiation patterns of the scattering waves decomposed into the modes for the spectra.

Keywords: Scattering problem; Elastic layered half space; Eigenfunction expansion form of the Green's function

1. Introduction

The analysis of scattering waves due to a scattering object and a plane incident wave in an elastic layered half space is an important issue in the identification of energy resources, site characterization and earthquake engineering. The analysis becomes possible by means of the Green's function for an elastic layered half space and the boundary integral equation method. Few researches have addressed the scattering problem in a layered medium (for example, Touhei, 2000), while a number of projects have investigated

E-mail address: touhei@rs.noda.tus.ac.jp (T. Touhei).

0020-7683/03/$ - see front matter © 2003 Elsevier Science Ltd. All rights reserved.
doi:10.1016/S0020-7683(03)00157-4

Green's function for an elastic layered half space. This is because analysis of the scattering problem is difficult due to the complicated representation of Green's function for an elastic layered medium.

Techniques to investigate Green's functions for an elastic layered medium include the reflectivity method (Fuchs and Müller, 1971), the discrete wavenumber method (Bouchon and Aki, 1977; Bouchon, 1979–1982), the normal mode superposition method (Harvey, 1981), and Green's function represented by leaky modes (Haddon, 1984, 1986, 1987). In addition, a method without the problem of growing exponential terms in Green's function was presented by Kenet and Kerry (1979) and the complex poles in the permissible sheets for Green's function were investigated by Watson (1972). A significant amount of literature has also been published on the scattering problem. The effects of cracks on scattering waves in a three-dimensional half space were analyzed by Budreck and Achenbach (1989) and the application of integral equation methods to the scattering and inverse scattering problems were shown by Colton and Kress (1983, 1998).

The simplification of Green's function for a layered medium would greatly assist in its application to the scattering problem. One technique to simplify the formulation uses the eigenvalue problem for a layered medium. The reason for this is that it is possible to impose complicated information for a layered medium (i.e., material properties, layer interface conditions, etc.) on eigenfunctions. The purpose of this paper is to present the formulation and numerical examples of the analysis of scattering waves in an elastic layered half space based on the complete eigenfunction expansion form of the Green's function developed by the author (Touhei, 2002a). The Green's function used here is an extension of that represented by the residue terms and the branch line integrals given by Lamb (1904). The present expression, however, clarifies the mathematical common frame between the residue terms and the branch line integrals with respect to the eigenfunctions and energy integrals. The advantage of the complete eigenfunction expansion form of the Green's function for the analysis is that the formulation itself becomes independent of the number of layers and the scattering waves can be decomposed into the modes for the spectra for the layered medium, which aids in the understanding of the properties of the scattering waves.

The work presented here is an extension of the result for an acoustic layered half space (Touhei, 2000, 2002b). However, the extension is not straightforward. In the first part of this paper, the complete eigenfunction expansion form of the Green's function applicable to the scattering problem is presented. This form of the Green's function provides the understanding of the properties of the k^{-1} singularity of the horizontal wavefunction for the eigenfunction expansion form of the Green's function at $k = 0$, where k is the wavenumber. Namely, the singularity does not have any effect on the Green's function. As a result, the Green's function is found to be simply expressed by the summation and integration of the eigenfunctions for the spectra for the layered medium. In addition, a proof is presented for the fact that the complex Rayleigh wave modes for the Green's function show standing waves. Next, the boundary integral equation for the scattering problem is presented based on the Green's functions. A method for decomposing scattering waves into eigenfunctions for an elastic layered medium is also explained. The decomposition is performed by interchanging the operation required for the boundary integral with that for composing the Green's functions. Finally, several numerical calculations are shown to verify the proposed method as well as to investigate the spectral structure and radiation patterns of the scattering wave.

2. Definition of the problem

Fig. 1 shows the concept of the scattering problem presented in this paper. A scattering object is embedded in an elastic layered half space and a plane incident wave is propagating in the medium. Scattering waves are caused by interaction between the object and the plane incident wave. The time factor used to express progressive waves is set at $\exp(\mathrm{i}\omega t)$, where t is time and ω is the circular frequency. Scattering waves are analyzed here in the frequency domain. As shown in Fig. 1, the vertical axis is denoted by x_3. Occa-

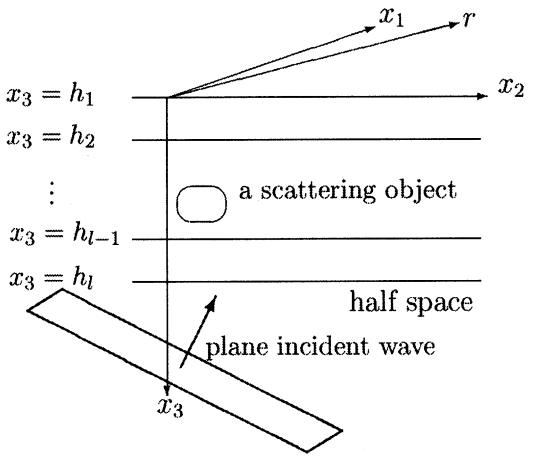

Fig. 1. The concept of the scattering problem. A scattering object is embedded in an elastic layered half space and a plane incident wave propagates in the layered medium.

sionally, x_3 is replaced by z for the sake of convenience. The layer indices attached to the variable h express the vertical coordinate of the layer interfaces. Note that $z = h_1(= 0)$ denotes the free surface of the layered medium.

A cartesian coordinate system is employed for the formulation except for the investigation of the properties of the Green's function for the layered medium, in which a cylindrical coordinate system is used. The variable $\boldsymbol{r}$ is used to express the spatial point. In cases in which a cartesian coordinate system is used, the components of $\boldsymbol{r}$ are denoted by $\boldsymbol{r} = (x_1, x_2, x_3)$, where x_1 and x_2 are the horizontal coordinates. For the cylindrical coordinate system, the components of $\boldsymbol{r}$ are denoted by $\boldsymbol{r} = (r, \theta, z)$.

The propagation of elastic waves in a layered medium due to a plane incident wave is governed by the following equation:

$$[(\lambda + \mu)\nabla\nabla\cdot + \mu\nabla^2 + \rho\omega^2]\boldsymbol{u}(\boldsymbol{r}) = \boldsymbol{0}, \quad \boldsymbol{r} = (x_1, x_2, x_3) \in R^2 \times R_+ \setminus (\Omega \cup \Gamma) \tag{1}$$

where ρ, λ and μ denote the mass density and Lamé constants respectively, $\boldsymbol{u}$ is the displacement field whose components are expressed by

$$\boldsymbol{u} = (u_1, u_2, u_3)^{\mathrm{T}}$$

Ω is the region inside the scattering object and Γ is its boundary. Note that the mass density and Lamé constants describing the properties of the layered medium are positive, bounded and piecewise constant functions with respect to each layer. In the following discussion, the wavenumbers

$$\begin{aligned} k_T &= \frac{\omega}{\sqrt{\mu/\rho}} \\ k_L &= \frac{\omega}{\sqrt{(\lambda + 2\mu)/\rho}} \end{aligned} \tag{2}$$

are used, where k_T and k_L are the wavenumber for the S and P waves, respectively, which are also the piecewise constant functions with respect to each layer.

At the interfaces of the layered medium, the displacements and the tractions satisfy the following layer interface conditions:

$$\begin{aligned} &u_\alpha(x_1,x_2,h_j-\epsilon)=u_\alpha(x_1,x_2,h_j+\epsilon)\\ &n_\beta^{(\mathrm{lay})}\tau_{\alpha\beta}(x_1,x_2,h_j-\epsilon)=n_\beta^{(\mathrm{lay})}\tau_{\alpha\beta}(x_1,x_2,h_j+\epsilon)\quad (j=1,2,\ldots,) \end{aligned} \tag{3}$$

where ϵ is an infinitesimally small positive number, the Greek characters indicate the components of a vector or tensor for which the summation convention is applied, $\tau_{\alpha\beta}$ is the component of the stress tensor and $n_\beta^{(\mathrm{lay})}$ is that of the normal vector of the layer interface. The component of the stress tensor is given by

$$\tau_{\alpha\beta}=\lambda\delta_{\alpha\beta}\partial_\gamma u_\gamma+\mu(\partial_\beta u_\alpha+\partial_\alpha u_\beta) \tag{4}$$

where $\delta_{\alpha\beta}$ denotes the Kronecker delta and ∂ is the partial differential operator whose subscript denotes the parameter for differentiation. The free boundary condition for the layered medium is expressed by

$$n_\beta^{(\mathrm{lay})}\tau_{\alpha\beta}(x_1,x_2,h_1)=0 \tag{5}$$

The scattering object here is assumed to be an elastic homogeneous medium. The equation of motion inside the scattering object is given as

$$[(\lambda^{(i)}+\mu^{(i)})\nabla\nabla\cdot+\mu^{(i)}\nabla^2+\rho^{(i)}\omega^2]\boldsymbol{u}^{(i)}(\boldsymbol{r})=\boldsymbol{0},\quad \boldsymbol{r}=(x_1,x_2,x_3)\in\Omega \tag{6}$$

where the superscript (i) denotes that the variables are for the inclusion of the scattering object. At the boundary of the scattering object, the following interface conditions have to be imposed:

$$\begin{aligned} &u_\alpha(\boldsymbol{r})=u_\alpha^{(i)}(\boldsymbol{r})\\ &n_\beta^{(\Gamma)}\tau_{\alpha\beta}(\boldsymbol{r})=n_\beta^{(\Gamma)}\tau_{\alpha\beta}^{(i)}(\boldsymbol{r})\quad (\boldsymbol{r}\in\Gamma) \end{aligned} \tag{7}$$

where $n_\beta^{(\Gamma)}$ is the normal vector of unit length at the boundary of the scattering object. The direction of the normal vector is away from the object.

Analysis of scattering waves becomes possible by solving Eqs. (1) and (6) under the conditions shown in Eqs. (3), (5) and (7). In this paper, Eqs. (1) and (6) are modified into boundary integral equations, which are coupled by means of Eq. (7). The complete eigenfunction expansion form of the Green's function (Touhei, 2002a) is used for Eq. (1), such that Eqs. (3) and (5) are automatically satisfied.

3. Complete eigenfunction expansion form of the Green's function

The boundary integral equation method requires Green's functions for both displacement and traction. The purpose of this section is to present the complete eigenfunction expansion form of Green's functions for displacement and traction. For this purpose, the formulation here begins with the direct wavenumber integral representation of Green's functions due to single and double sources. The cylindrical coordinate system is mainly employed here, in which the array of the components for the vector is such that

$$\boldsymbol{u}=(u_z\quad u_r\quad u_\theta)^{\mathrm{T}} \tag{8}$$

due to the Fourier–Hankel transform shown in Appendix A. The transformation of the coordinate from the cylindrical to cartesian coordinate systems is also provided for the boundary integral equation.

3.1. The Green's function represented by the direct wavenumber integral

First of all, we define the Green's function due to single and double sources in an elastic layered half space. Let $\boldsymbol{s}(r,\theta)$ and $\boldsymbol{d}_\beta(r,\theta)$ $(\beta=1,2)$ be the single and double source, respectively, which are defined by

$$
\begin{aligned}
\boldsymbol{s}(r,\theta) &= \mathbf{1}\frac{\delta(r)}{r}\delta(\theta) \\
\boldsymbol{d}_1(r,\theta) &= \frac{\mathbf{1}}{\epsilon}\left(\frac{\delta(r-\epsilon/2)}{r}\delta(\theta) - \frac{\delta(r-\epsilon/2)}{r}\delta(\theta-\pi)\right) \\
\boldsymbol{d}_2(r,\theta) &= \frac{\mathbf{1}}{\epsilon}\left(\frac{\delta(r-\epsilon/2)}{r}\delta(\theta-\pi/2) - \frac{\delta(r-\epsilon/2)}{r}\delta(\theta+\pi/2)\right)
\end{aligned}
\tag{9}
$$

where $\mathbf{1}$ is the identity matrix, the subscript β for the double source indicates the axis along which the double source is applied and $\delta(\cdot)$ is the Dirac delta function. The locations of the double sources are explained by Fig. 2. The Green's functions due to the sources are defined by

$$
\begin{aligned}
&[(\lambda+\mu)\nabla\nabla\cdot + \mu\nabla^2 + \rho\omega^2]\boldsymbol{G}(\boldsymbol{r}) = -\boldsymbol{s}(r,\theta)\delta(z-z') \\
&[(\lambda+\mu)\nabla\nabla\cdot + \mu\nabla^2 + \rho\omega^2]\boldsymbol{T}_\beta(\boldsymbol{r}) = -\boldsymbol{d}_\beta(r,\theta)\delta(z-z') \quad (\beta = 1,2)
\end{aligned}
\tag{10}
$$

where $\boldsymbol{r} \in R^2 \times R_+$, $\boldsymbol{G}$ and $\boldsymbol{T}_\beta$ are the Green's functions due to the single source and double sources, respectively, and z' is the vertical coordinate of the source point. Let $\hat{\boldsymbol{s}}_k^m$ and $\hat{\boldsymbol{d}}_{\beta k}^m$ be the Fourier–Hankel transform of $\boldsymbol{s}$ and $\boldsymbol{d}_\beta$, respectively. According to the Fourier–Hankel transform, $\hat{\boldsymbol{s}}_k^m$ and $\hat{\boldsymbol{d}}_{\beta k}^m$ are obtained from

$$
\hat{\boldsymbol{s}}_k^m = \int_0^{2\pi} \mathrm{d}\theta \int_0^\infty r\boldsymbol{H}_k^m(r,-\theta)\boldsymbol{s}(r,\theta)\,\mathrm{d}r \tag{11}
$$

$$
\hat{\boldsymbol{d}}_{\beta k}^m = \int_0^{2\pi} \mathrm{d}\theta \int_0^\infty r\boldsymbol{H}_k^m(r,-\theta)\boldsymbol{d}_\beta(r,\theta)\,\mathrm{d}r \tag{12}
$$

where k is the horizontal wavenumber, m is the circumferential order number and $\boldsymbol{H}_k^m$ is the horizontal wavefunction defined by Eq. (A.4). It is not difficult to show the followings due to a property of the Bessel functions:

$$
\begin{aligned}
&\hat{\boldsymbol{s}}_k^m = \mathbf{0} \quad (|m| \geqslant 2) \\
&\hat{\boldsymbol{d}}_{\beta k}^m = \mathbf{0} \quad (\beta = 1,2), \quad (|m| \geqslant 3)
\end{aligned}
\tag{13}
$$

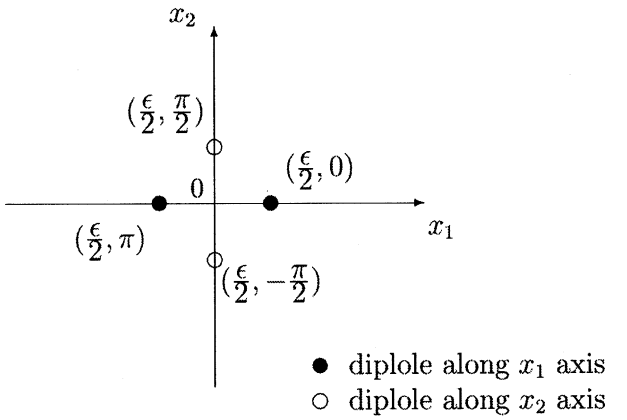

Fig. 2. Dipoles along x_1- and x_2-axes to calculate the derivative of Green's function. A cylindrical coordinate system is used to indicate the positions.

Therefore, the solutions for Eq. (10) are expressed by the finite series for m that are as follows:

$$\begin{aligned}\boldsymbol{G}(\boldsymbol{r}) &= \frac{1}{2\pi}\sum_{m=-1}^{1}\int_0^\infty k\boldsymbol{H}_k^m(r,\theta)\widehat{\boldsymbol{G}}_k^m(z)\,\mathrm{d}k \\ \boldsymbol{T}_\beta(\boldsymbol{r}) &= \frac{1}{2\pi}\sum_{m=-2}^{2}\int_0^\infty k\boldsymbol{H}_k^m(r,\theta)\widehat{\boldsymbol{T}}_{\beta k}^m(z)\,\mathrm{d}k \quad (\beta=1,2)\end{aligned} \tag{14}$$

where $\widehat{\boldsymbol{G}}_k^m$ and $\widehat{\boldsymbol{T}}_{\beta k}^m$ are the Fourier–Hankel transform of $\boldsymbol{G}$ and $\boldsymbol{T}$, respectively, which are obtained from the following:

$$\begin{aligned}\mathscr{A}_k\widehat{\boldsymbol{G}}_k^m(z) &= \hat{\boldsymbol{s}}_k^m\delta(z-z') \\ \mathscr{A}_k\widehat{\boldsymbol{T}}_{\beta k}^m(z) &= \hat{\boldsymbol{d}}_{\beta k}^m\delta(z-z') \quad (\beta=1,2)\end{aligned} \tag{15}$$

Note that $\mathscr{A}_k$ is the differential operator with components

$$\mathscr{A}_k = \begin{bmatrix} (\lambda+2\mu)\partial_z^2+\rho\omega^2-\mu k^2 & -(\lambda+\mu)k\partial_z & 0 \\ (\lambda+\mu)k\partial_z & \mu\partial_z^2+\rho\omega^2-(\lambda+2\mu)k^2 & 0 \\ 0 & 0 & \mu\partial_z^2+\rho\omega^2-\mu k^2 \end{bmatrix} \tag{16}$$

By means of the Green's function in the wavenumber domain, the solution for Eq. (15) is expressed as follows:

$$\begin{aligned}\widehat{\boldsymbol{G}}_k^m(z) &= \boldsymbol{g}_k(z,z')\hat{\boldsymbol{s}}_k^m \\ \widehat{\boldsymbol{T}}_{\beta k}^m(z) &= \boldsymbol{g}_k(z,z')\hat{\boldsymbol{d}}_{\beta k}^m \quad (\beta=1,2)\end{aligned} \tag{17}$$

where $\boldsymbol{g}_k(z,z')$ is the Green's function in the wavenumber domain for which the method of composition is given in Appendix B. Substitution of Eq. (17) into Eq. (14) leads to the following representation of the solutions of Eq. (10):

$$\begin{aligned}\boldsymbol{G}(\boldsymbol{r}) &= \frac{1}{2\pi}\sum_{m=-1}^{1}\int_0^\infty k\boldsymbol{H}_k^m(r,\theta)\boldsymbol{g}_k(z,z')\hat{\boldsymbol{s}}_k^m\,\mathrm{d}k \\ \boldsymbol{T}_\beta(\boldsymbol{r}) &= \frac{1}{2\pi}\sum_{m=-2}^{2}\int_0^\infty k\boldsymbol{H}_k^m(r,\theta)\boldsymbol{g}_k(z,z')\hat{\boldsymbol{d}}_{\beta k}^m\,\mathrm{d}k \quad (\beta=1,2)\end{aligned} \tag{18}$$

Appendix B shows the asymptotic property of the Green's function in the wavenumber domain:

$$\boldsymbol{g}_k(z,z') = \mathrm{O}(k^{-\alpha}\exp(-k|z-z'|)) \quad (\alpha>0), \quad (k\to\infty) \tag{19}$$

where O is the Landau notation, which ensures the convergence of the wavenumber integrals shown in Eq. (18) for the case of $z\neq z'$.

3.2. Derivation of the complete eigenfunction expansion form of the Green's function

The derivation of the complete eigenfunction expansion form of the Green's function here relies on properties of the Green's function in the wavenumber domain. As shown in Appendix B, the permissible sheets for the Green's function in the wavenumber domain is the set of the complex wavenumbers such that

$$\mathscr{C} = \{k;\mathrm{Re}(\gamma_l)>0 \text{ and } \mathrm{Re}(\nu_l)>0\} \tag{20}$$

and the set of the wavenumbers for the branch cut is

$$\sigma_\mathrm{c} = \{k;\mathrm{Re}(\gamma_l)=0\}\cup\{k;\mathrm{Re}(\nu_l)=0\} \tag{21}$$

where

$$\gamma_l = \sqrt{k^2 - k_{L(l)}^2}$$
$$\nu_l = \sqrt{k^2 - k_{T(l)}^2} \tag{22}$$

Note that $k_{L(l)}$ and $k_{T(l)}$ are the wavenumbers for the P and S waves in the half space, respectively. Some assumptions are imposed on the properties of the Green's function in the wavenumber domain in this paper. These assumptions are as follows:

Assumption 1. Let σ_{p} the set of wavenumbers for the poles of $\boldsymbol{g}_k(z,z')$. Then

$$\sigma_{\mathrm{p}} \subset \mathscr{C} \tag{23}$$

and all poles are simple.

The set σ_{p} consists of two parts. One is the normal modes which can be found on the real axis of the complex wavenumber plane. The other is the complex Rayleigh wave modes representing all the permissible sheets. The presence of the complex Rayleigh wave modes is acknowledged by the work of Watson (1972), in which the modes were found from numerical results to be distributed on a line close to the imaginary axis of the complex wavenumber plane. The next assumption is for the number of the normal modes and the complex Rayleigh wave modes.

Assumption 2. The number of normal modes is finite, while the complex Rayleigh wave modes are at most countable.

The derivation of the complete eigenfunction form of the Green's function due to a single source is shown here. The treatment for the Green's function due to a double source is similar, in that the details of the derivation process are omitted. To obtain the result, replace the horizontal wavefunction with

$$\boldsymbol{H}_k^m(r,\theta) = \tfrac{1}{2}[\boldsymbol{H}_k^{m(1)}(r,\theta) + \boldsymbol{H}_k^{m(2)}(r,\theta)] \tag{24}$$

where $\boldsymbol{H}_k^{m(1)}(r,\theta)$ and $\boldsymbol{H}_k^{m(2)}(r,\theta)$ are the horizontal wavefunctions constituted by

$$Y_k^{m(\tau)}(r,\theta) = H_m^{(\tau)}(kr)\exp(\mathrm{i}m\theta) \quad (\tau = 1,2)$$

Note that $H_m^{(\tau)}(\cdot)$ is the Hankel function of order m. Given the properties of the Hankel function, the following equations can be established:

$$\int_\epsilon^\infty k\boldsymbol{H}_k^{m(1)}(r,\theta)\boldsymbol{g}_k(z,z')\hat{\boldsymbol{s}}_k^m \,\mathrm{d}k = \int_{M_1+C_1} k\boldsymbol{H}_k^{m(1)}(r,\theta)\boldsymbol{g}_k^{\downarrow}(z,z')\hat{\boldsymbol{s}}_k^m \,\mathrm{d}k + 2\pi\mathrm{i}\sum_{k_j\in\sigma_{\mathrm{p}l}^*} \operatorname*{Res}_{k=k_j}[k\boldsymbol{H}_k^{m(1)}(r,\theta)\boldsymbol{g}_k(z,z')\hat{\boldsymbol{s}}_k^m] \tag{25}$$

$$\begin{aligned}\int_\epsilon^\infty k\boldsymbol{H}_k^{m(2)}(r,\theta)\boldsymbol{g}_k(z,z')\hat{\boldsymbol{s}}_k^m \,\mathrm{d}k = {} & \int_{N_1} k\boldsymbol{H}_k^{m(2)}(r,\theta)\boldsymbol{g}_k^{\downarrow}(z,z')\hat{\boldsymbol{s}}_k^m \,\mathrm{d}k + \int_{N_2+C_3+M_3} k\boldsymbol{H}_k^{m(2)}(r,\theta)\boldsymbol{g}_k^{\uparrow}(z,z')\hat{\boldsymbol{s}}_k^m \,\mathrm{d}k \\ & - 2\pi\mathrm{i}\sum_{k_j\in\sigma_{\mathrm{p}l}} \operatorname*{Res}_{k=k_j}[k\boldsymbol{H}_k^{m(2)}(r,\theta)\boldsymbol{g}_k(z,z')\hat{\boldsymbol{s}}_k^m] \\ & - 2\pi\mathrm{i}\sum_{k_n\in\sigma_{\mathrm{p}n}} \operatorname*{Res}_{k=k_n}[k\boldsymbol{H}_k^{m(2)}(r,\theta)\boldsymbol{g}_k(z,z')\hat{\boldsymbol{s}}_k^m]\end{aligned} \tag{26}$$

where the integration paths C_1, M_1, C_3, N_1, N_2 and M_3 are shown in Figs. 3 and 4, $\sigma_{\mathrm{p}n}$ is the set of wavenumbers for the normal modes on the positive real axis, $\sigma_{\mathrm{p}l}^*$ is the set of wavenumbers of the complex

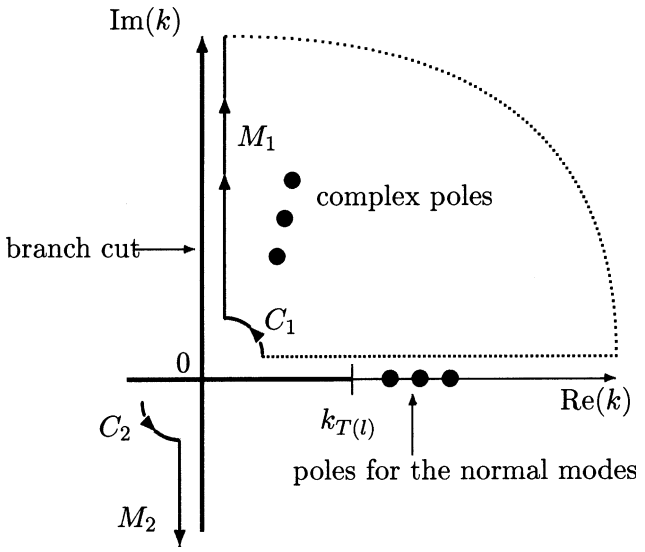

Fig. 3. Integral paths for M_1, M_2, C_1 and C_2.

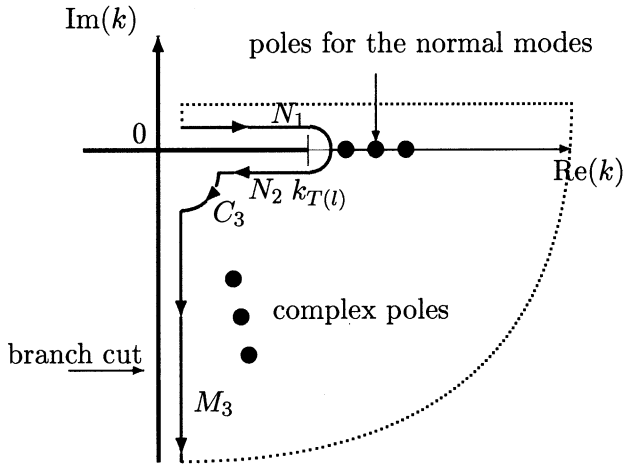

Fig. 4. Integral paths for N_1, N_2, M_3 and C_3.

Rayleigh wave modes located in the first quadrant of the complex wavenumber plane and σ_{pl} is the set of those in the fourth quadrant.

Note that integration paths C_1 and C_3 are necessary due to the singularity of the horizontal wavefunction. A brief sketch of the location of the wavenumbers for those modes is shown in Figs. 3 and 4. The superscripts $\uparrow$ and $\downarrow$ for the Green's function in the wavenumber domain refer to the direction of the wave propagation in the half space. Namely, $\uparrow$ denotes an up-going wave and $\downarrow$ a down-going wave.

Next, replace $k = -k'$ for the integration paths of C_1 and M_1. The properties of the Bessel functions (McLachlan, 1961) shown below

$$\begin{aligned} J_m(-kr) &= \exp(\mathrm{i}m\pi)J_m(kr) \\ H_m^{(1)}(-kr) &= \exp(\mathrm{i}(m+1)\pi)H_m^{(2)}(kr) \quad (\text{for } -\pi < \mathrm{Arg}\, k < 0) \end{aligned} \tag{27}$$

and the following property of the Green's function in the wavenumber domain clarified by the propagator matrix method shown in Appendix B:

$$\boldsymbol{g}_{-k}(z,z') = \mathrm{diag}[1,-1,-1]\boldsymbol{g}_k(z,z')\,\mathrm{diag}[1,-1,-1] \tag{28}$$

leads to the following equation:

$$\int_{\epsilon}^{\infty} k\boldsymbol{H}_k^{m(1)}(r,\theta)\boldsymbol{g}_k(z,z')\hat{\boldsymbol{s}}_k^m\,\mathrm{d}k = -\int_{M_2+C_2} k'\boldsymbol{H}_{k'}^{m(2)}(r,\theta)\boldsymbol{g}_{k'}^{\downarrow}(z,z')\hat{\boldsymbol{s}}_{k'}^m\,\mathrm{d}k' + 2\pi\mathrm{i}\sum_{k_j\in\sigma_{\mathrm{p}l}}\operatorname*{Res}_{k=k_j}[k\boldsymbol{H}_k^{m(1)}(r,\theta)\boldsymbol{g}_k(z,z')\hat{\boldsymbol{s}}_k^m] \tag{29}$$

where the integration paths C_2 and M_2 are shown in Fig. 3.

The complete eigenfunction expansion form of the Green's function is obtained by adding Eqs. (26) and (29). For this operation, let us define the set of wavenumbers $\sigma_{\mathrm{p}+}$ such that

$$\sigma_{\mathrm{p}+} = \sigma_{\mathrm{p}n} \cup \sigma_{\mathrm{p}l} \cup \sigma_{\mathrm{p}l}^* \tag{30}$$

The set $\sigma_{\mathrm{p}+}$ is the subset of the discrete spectrum σ_{p}. In addition, define the subset of the wavenumbers for the branch cuts in the complex wavenumber plane located in positive real and negative imaginary axes. This set is expressed by $\sigma_{\mathrm{c}+}$, which is the subset of the continuous spectrum σ_{c}. A brief sketch of the location of these spectra is shown in Fig. 5. Presence of the eigenfunctions can be observed for the wavenumbers of the spectra. The eigenfunctions for the continuous spectrum are not in L_2 space and are therefore called improper eigenfunctions. The following theorems (Touhei, 2002a) are also incorporated into the operation for the addition of Eqs. (26) and (29):

Theorem 1. *Let $k_j \in \sigma_{\mathrm{p}}$. Then, the residue of the Green's function in the wavenumber domain at wavenumber k_j is decomposed into the eigenfunction such that*

$$\operatorname*{Res}_{k=k_j}\boldsymbol{g}_k(z,z') = \frac{1}{2}\boldsymbol{\Psi}_{k_j}(z)\boldsymbol{E}_{k_j}^{-1}\boldsymbol{\Psi}_{k_j}(z')^{\mathrm{T}} \quad (k_j \in \sigma_{\mathrm{p}}) \tag{31}$$

where $\boldsymbol{\Psi}_{k_j}(z)$ is the eigenfunction and $\boldsymbol{E}_{k_j}$ is the energy integral defined for the discrete spectrum σ_{p}.

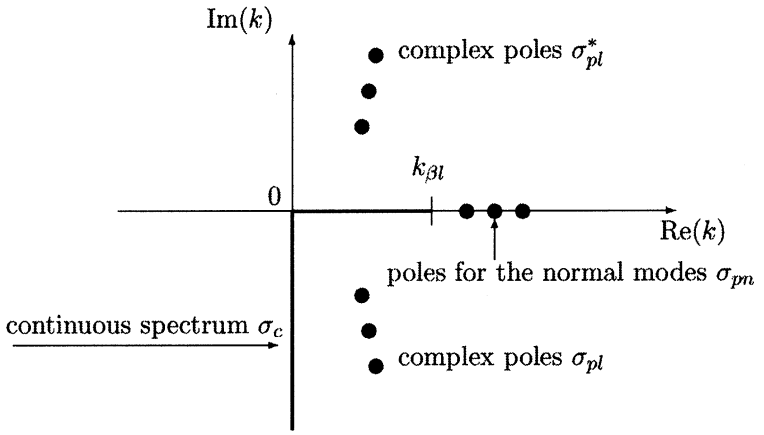

Fig. 5. Location of the spectra in the complex wavenumber plane.

Theorem 2. *The discontinuity of the Green's function in the wavenumber domain at the branch cuts can be decomposed into the improper eigenfunction as follows:*

$$\boldsymbol{g}_k^{\uparrow}(z,z') - \boldsymbol{g}_k^{\downarrow}(z,z') = \pi \mathrm{i} \frac{k}{|k|} \boldsymbol{\Psi}_k(z) \boldsymbol{E}_k^{-1} \boldsymbol{\Psi}_k(z')^{\mathrm{T}} \quad (k \in \sigma_{\mathrm{c}}) \tag{32}$$

where $\boldsymbol{\Psi}_k(z)$ is the improper eigenfunction and $\boldsymbol{E}_k$ is the energy integral defined for the continuous spectrum σ_{c}.

The definition of the energy integral for the discrete spectrum is

$$\boldsymbol{E}_k = k \int_0^{\infty} \boldsymbol{\Psi}_k(z)^{\mathrm{T}} \boldsymbol{K}_2 \boldsymbol{\Psi}_k(z) \, \mathrm{d}z + \int_0^{\infty} \partial_z \boldsymbol{\Psi}_k(z)^{\mathrm{T}} \boldsymbol{K}_3 \boldsymbol{\Psi}_k(z) \, \mathrm{d}z \quad (k \in \sigma_{\mathrm{p}}) \tag{33}$$

while that for the continuous spectrum is

$$\boldsymbol{E}_k \delta(|\xi| - |k|) = k \int_0^{\infty} \boldsymbol{\Psi}_{\xi}(z)^{\mathrm{T}} \boldsymbol{K}_2 \boldsymbol{\Psi}_k(z) \, \mathrm{d}z + \int_0^{\infty} \partial_z \boldsymbol{\Psi}_{\xi}(z)^{\mathrm{T}} \boldsymbol{K}_3 \boldsymbol{\Psi}_k(z) \, \mathrm{d}z + \mathrm{O}(1) \quad (\xi, k \in \sigma_{\mathrm{c}}) \tag{34}$$

where $\boldsymbol{K}_2$ and $\boldsymbol{K}_3$ are denoted by

$$\begin{aligned} \boldsymbol{K}_2 &= \mathrm{diag}[\mu \quad (\lambda + 2\mu) \quad \mu] \\ \boldsymbol{K}_2 &= \begin{bmatrix} 0 & -\lambda & 0 \\ \mu & 0 & 0 \\ 0 & 0 & 0 \end{bmatrix} \end{aligned} \tag{35}$$

The integration of Eq. (34) is for the improper eigenfunctions that are not in L_2 space, so that the Dirac delta function is required to express the divergence of the integral. In addition, the Landau notation O(1) in Eq. (34) represents a term which remains constant when ξ approaches k. The energy integrals are symmetry matrices (Touhei, 2002a) which ensures the reciprocity of the Green's function.

The addition of Eqs. (26) and (29) leads to the following:

$$\begin{aligned} \boldsymbol{G}(\boldsymbol{r}) = &-\frac{\mathrm{i}}{4} \sum_{m=-1}^{1} \sum_{k \in \sigma_{\mathrm{p}}} s(k) k \boldsymbol{H}_k^{m(\tau)}(r,\theta) \boldsymbol{\Psi}_k(z) \boldsymbol{E}_k^{-1} \boldsymbol{\Psi}_k(z')^{\mathrm{T}} \hat{\boldsymbol{s}}_k^m \\ &-\frac{\mathrm{i}}{4} \sum_{m=-1}^{1} \int_{\sigma_{\mathrm{c}}} k \boldsymbol{H}_k^{m(\tau)}(r,\theta) \boldsymbol{\Psi}_k(z) \boldsymbol{E}_k^{-1} \boldsymbol{\Psi}_k(z')^{\mathrm{T}} \hat{\boldsymbol{s}}_k^m \, |\mathrm{d}k| + \boldsymbol{B}_{\mathrm{s}}(\boldsymbol{r}) \end{aligned} \tag{36}$$

where $s(k)$ is the function

$$s(k) = \begin{cases} 1 & \text{when } k \in \sigma_{\mathrm{p}n} \cup \sigma_{\mathrm{p}l} \\ -1 & \text{when } k \in \sigma_{\mathrm{p}l}^* \end{cases} \tag{37}$$

τ takes 1 or 2 according to k as follows:

$$\tau = \begin{cases} 2 & \text{when } k \in \sigma_{\mathrm{p}n} \cup \sigma_{\mathrm{p}l} \\ 1 & \text{when } k \in \sigma_{\mathrm{p}l}^* \end{cases} \tag{38}$$

In addition $\boldsymbol{B}_{\mathrm{s}}(\boldsymbol{r})$ is due to the singularity of the horizontal wavefunction at $k = 0$, which can be expressed as

$$\boldsymbol{B}_{\mathrm{s}}(\boldsymbol{r}) = \frac{1}{2\pi} \sum_{m=-1}^{1} \int_{C_2+C_3} k \boldsymbol{H}_k^{m(2)}(r,\theta) \boldsymbol{g}_k(z,z') \hat{\boldsymbol{s}}_k^m \, \mathrm{d}k \tag{39}$$

A similar procedure is available for the Green's function due to a double source. The result is as follows:

$$\boldsymbol{T}_\beta(\boldsymbol{r}) = -\frac{\mathrm{i}}{4}\sum_{m=-2}^{2}\sum_{k\in\sigma_\mathrm{p}} s(k)k\boldsymbol{H}_k^{m(\tau)}(r,\theta)\boldsymbol{\Psi}_k(z)\boldsymbol{E}_k^{-1}\boldsymbol{\Psi}_k(z')^{\mathrm{T}}\hat{\boldsymbol{d}}_{\beta k}^m - \frac{\mathrm{i}}{4}\sum_{m=-2}^{2}\int_{\sigma_\mathrm{c}} k\boldsymbol{H}_k^{m(\tau)}(r,\theta)\boldsymbol{\Psi}_k(z)\boldsymbol{E}_k^{-1}\boldsymbol{\Psi}_k(z')^{\mathrm{T}}\hat{\boldsymbol{d}}_{\beta k}^m\,|\mathrm{d}k| + \boldsymbol{B}_{\mathrm{d}\beta}(\boldsymbol{r}) \tag{40}$$

The effects of the singularity of the horizontal wavefunction at $k=0$ for Eq. (40) is expressed by $\boldsymbol{B}_{\mathrm{d}\beta}(\boldsymbol{r})$ which is as follows:

$$\boldsymbol{B}_{\mathrm{d}\beta}(\boldsymbol{r}) = \frac{1}{2\pi}\sum_{m=-2}^{2}\int_{C_2+C_3} k\boldsymbol{H}_k^{m(2)}(r,\theta)\boldsymbol{g}_k(z,z')\hat{\boldsymbol{d}}_{\beta k}^m\,\mathrm{d}k \tag{41}$$

3.3. Singularity of the horizontal wavefunction

In this section, the effects of the singularity of the horizontal wavefunction $\boldsymbol{B}_\mathrm{s}(\boldsymbol{r})$ and $\boldsymbol{B}_{\mathrm{d}\beta}(\boldsymbol{r})$ shown in Eqs. (39) and (41) are clarified. The singularity around $k\sim 0$ of the Hankel function used in the horizontal wavefunction becomes stronger as m increases. Assuming that $m\geqslant 1$, the principal part of the singularity of the horizontal wavefunction at $k=0$ becomes

$$\boldsymbol{H}_k^{m(2)}(r,\theta) \underset{k\to 0}{\sim} \frac{2^m(m-1)!}{\pi}\mathrm{i}\mathrm{e}^{\mathrm{i}m\theta}(kr)^{-m}\begin{bmatrix}1 & 0 & 0\\ 0 & -m(kr)^{-1} & \mathrm{i}m(kr)^{-1}\\ 0 & \mathrm{i}m(kr)^{-1} & m(kr)^{-1}\end{bmatrix} \tag{42}$$

On the other hand, in the case that $m=1$, $\hat{\boldsymbol{s}}_k^m$ for the Green's function due to the single source is

$$\hat{\boldsymbol{s}}_k^m = \begin{bmatrix}0 & 0 & 0\\ 0 & 1/2 & (-1/2)\mathrm{i}\\ 0 & (-1/2)\mathrm{i} & -1/2\end{bmatrix} \tag{43}$$

Therefore, according to Eqs. (42) and (43), the integrand of Eq. (39) shows k^{-1} singularity around $k\sim 0$ in the case that $m=1$. To evaluate the singularity, the Green's function in the wavenumber domain around $k\sim 0$ must be investigated. The operator $\mathscr{A}_k$ for the Green's function in the wavenumber domain defined in Eq. (16) has the following property:

$$\mathscr{A}_k \underset{k\to 0}{\longrightarrow} \begin{bmatrix}(\lambda+2\mu)\partial_z^2+\rho\omega^2 & 0 & 0\\ 0 & \mu\partial_z^2+\rho\omega^2 & 0\\ 0 & 0 & \mu\partial_z^2+\rho\omega^2\end{bmatrix} \tag{44}$$

Therefore, the Green's function in the wavenumber domain shows

$$\boldsymbol{g}_k(z,z') \underset{k\to 0}{\longrightarrow} \mathrm{diag}[\alpha(z,z'),\beta(z,z'),\beta(z,z')] \tag{45}$$

where

$$((\lambda+2\mu)\partial_z^2+\rho\omega^2)\alpha(z,z') = -\delta(z-z')$$

$$(\mu\partial_z^2+\rho\omega^2)\beta(z,z') = -\delta(z-z')$$

A property of the integrand of Eq. (39) can now be summarized as follows by means of Eqs. (42), (43) and (45):

$$k\boldsymbol{H}_k^m(r,\theta)\boldsymbol{g}_k(z,z')\hat{\boldsymbol{s}}_k^m \underset{k\to 0}{\to} \begin{bmatrix} 0 & 0 & 0 \\ 0 & 0 & 0 \\ 0 & 0 & 0 \end{bmatrix} \tag{46}$$

Therefore, the singularity of k^{-1} due to the horizontal wavefunction does not affect the integration when $m = 1$. When $m \leqslant -1$, a property of the Hankel function

$$H_{-m}^{(\tau)}(\cdot) = (-1)^m H_m^{(\tau)}(\cdot)$$

ensures the possibility of the usage of the discussion presented here. It is clear that the singularity of k^{-1} is not an issue when $m = 0$. A similar procedure is possible for the Green's function due to a double source. The following theorem is a summary of the above discussion and the Green's function is found to be simply expressed in terms of only the normal, complex and improper modes.

Theorem 3. *The singularity of the horizontal wavefunction at $k = 0$ does not have any effect on Green's function. Namely,*

$$\boldsymbol{B}_{\mathrm{s}}(\boldsymbol{r}) = \frac{1}{2\pi}\sum_{m=-1}^{1}\int_{C_2+C_3} k\boldsymbol{H}_k^m(r,\theta)\boldsymbol{g}_k(z,z')\hat{\boldsymbol{s}}_k^m \,\mathrm{d}k = \boldsymbol{0}$$

$$\boldsymbol{B}_{\mathrm{d}\beta}(\boldsymbol{r}) = \frac{1}{2\pi}\sum_{m=-2}^{2}\int_{C_2+C_3} k\boldsymbol{H}_k^m(r,\theta)\boldsymbol{g}_k(z,z')\hat{\boldsymbol{d}}_{\beta k}^m \,\mathrm{d}k = \boldsymbol{0}$$

3.4. Properties of the complex Rayleigh wave modes

The fact that the imaginary part of the whole of the complex Rayleigh wave modes for the Green's function is zero has been shown (Touhei, 2002a). However, the proof for this was complicated. In this section, a simple proof for the fact is presented. Here, ζ is used for the complex variable and the superscript $*$ for the complex variable indicates the complex conjugate. The following lemma is required for the discussion:

Lemma 1. *There is a relationship between the first and second kind of Hankel function for the complex variables, which can be written as*

$$H_m^{(1)}(\zeta^*) = [H_m^{(2)}(\zeta)]^*$$

The proof was given in the article (Touhei, 2002a).

In addition, the following relationship for the first kind of the Bessel functions:

$$J_m(\zeta^*) = [J_m(\zeta)]^*$$

is also required for the discussion. One property of the horizontal wavefunctions, $\hat{\boldsymbol{s}}_k^m$ and $\hat{\boldsymbol{d}}_{\beta k}^m$ based on the above equations is

$$\begin{aligned} \boldsymbol{H}_{k^*}^{-m(1)}(r,\theta) &= (-1)^m[\boldsymbol{H}_k^{m(2)}(r,\theta)]^* \\ \hat{\boldsymbol{s}}_{k^*}^{-m} &= (-1)^m[\hat{\boldsymbol{s}}_k^m]^* \\ \hat{\boldsymbol{d}}_{\beta k^*}^{-m} &= (-1)^m[\hat{\boldsymbol{d}}_{\beta k}^m]^* \end{aligned} \tag{47}$$

In addition, note that

$$k \in \sigma_{\mathrm{p}l} \Longleftrightarrow k^* \in \sigma_{\mathrm{p}l}^*$$

and if $\boldsymbol{\Psi}_k(z)$ is the eigenfunction for the complex Rayleigh wave mode for the wavenumber k, then $(\boldsymbol{\Psi}_k(z))^*$ is also the eigenfunction for the complex Rayleigh wave mode for the wavenumber k^*. As a result, one property of the energy integral for the complex Rayleigh wave mode is such that

$$\boldsymbol{E}_{k^*} = (\boldsymbol{E}_k)^* \quad (k \in \sigma_{\mathrm{p}l})$$

The following theorem can now be presented:

Theorem 4. *The imaginary part of the whole of the complex Rayleigh wave modes in the Green's function is zero.*

Proof. Suppose that $k \in \sigma_{\mathrm{p}l}$. According to Eq. (36), superposition of the complex Rayleigh wave modes of the complex conjugate each other with the different signs of m leads to

$$\begin{aligned}&(-\mathrm{i}/4)\boldsymbol{H}_k^{m(2)}(r,\theta)\boldsymbol{\Psi}_k(z)\boldsymbol{E}_k^{-1}\boldsymbol{\Psi}_k(z')^{\mathrm{T}}\hat{\boldsymbol{s}}_k^m - (-\mathrm{i}/4)\boldsymbol{H}_{k^*}^{m(1)}(r,\theta)\boldsymbol{\Psi}_{k^*}(z)\boldsymbol{E}_{k^*}^{-1}\boldsymbol{\Psi}_{k^*}(z')^{\mathrm{T}}\hat{\boldsymbol{s}}_{k^*}^m \\ &\quad = (-\mathrm{i}/4)\boldsymbol{H}_k^{m(2)}(r,\theta)\boldsymbol{\Psi}_k(z)\boldsymbol{E}_k^{-1}\boldsymbol{\Psi}_k(z')^{\mathrm{T}}\hat{\boldsymbol{s}}_k^m - (-\mathrm{i}/4)[\boldsymbol{H}_k^{m(2)}(r,\theta)\boldsymbol{\Psi}_k(z)\boldsymbol{E}_k^{-1}\boldsymbol{\Psi}_k(z')^{\mathrm{T}}\hat{\boldsymbol{s}}_k^m]^*\end{aligned} \tag{48}$$

from which it is found that the imaginary part is zero. Therefore, the imaginary part of the whole complex Rayleigh wave mode is zero. A similar procedure is possible for the Green's function due to a double source. □

This theorem is valid for an arbitrary excitation frequency of real value. Therefore, the complex Rayleigh wave modes exhibit non-propagating waves, namely, standing waves, since the imaginary part of the wavefunction in the frequency domain is necessary to express a phase during wave propagation.

3.5. The Green's function for traction

It is now possible for us to transform the Green's function in the cylindrical coordinate system into that in a cartesian coordinate system. The transformation of the displacement vector at the field point becomes

$$\begin{pmatrix} u_1 \\ u_2 \\ u_3 \end{pmatrix} = \boldsymbol{R}(\theta)\begin{pmatrix} u_z \\ u_r \\ u_\theta \end{pmatrix} \tag{49}$$

where $\boldsymbol{R}(\theta)$ denotes

$$\boldsymbol{R}(\theta) = \begin{pmatrix} 0 & \cos\theta & -\sin\theta \\ 0 & \sin\theta & \cos\theta \\ 1 & 0 & 0 \end{pmatrix} \tag{50}$$

Likewise, the transformation of the force vector at the source point from the cartesian coordinate system into the cylindrical coordinate system is

$$\begin{pmatrix} f_z \\ f_r \\ f_\theta \end{pmatrix} = \boldsymbol{R}(0)^{\mathrm{T}}\begin{pmatrix} f_1 \\ f_2 \\ f_3 \end{pmatrix} \tag{51}$$

in case the horizontal coordinate of the source point is the origin of the coordinate system. Let the Green's function for displacement, namely, due to a single source, in the cartesian coordinate system be denoted by $\boldsymbol{U}(\boldsymbol{r},\boldsymbol{r}')$, where $\boldsymbol{r}'$ is the source point in which the horizontal coordinate are not the origin of the global coordinate system. The components of the field and source points in terms of the cartesian coordinate system are expressed by

$$\begin{aligned} \boldsymbol{r} &= (x_1, x_2, x_3) \\ \boldsymbol{r}' &= (x_1', x_2', x_3') \end{aligned} \tag{52}$$

Now, based on Eqs. (49) and (51), the Green's function can be expressed as follows:

$$\begin{aligned} \boldsymbol{U}(\boldsymbol{r}, \boldsymbol{r}') = &-\frac{\mathrm{i}}{4} \sum_{m=-1}^{1} \sum_{k \in \sigma_{\mathrm{p}+}} s(k) k \boldsymbol{\phi}_k^{m(\tau)}(x_1 - x_1', x_2 - x_2', x_3) \boldsymbol{E}_k^{-1} \boldsymbol{S}_k^m(x_3') \\ &-\frac{\mathrm{i}}{4} \sum_{m=-1}^{1} \int_{\sigma_{\mathrm{c}+}} k \boldsymbol{\phi}_k^m(x_1 - x_1', x_2 - x_2', x_3) \boldsymbol{E}_k^{-1} \boldsymbol{S}_k^m(x_3') |\mathrm{d}k| \end{aligned} \tag{53}$$

where $\boldsymbol{\phi}_k^m$ and $\boldsymbol{S}_k^m$ are defined by

$$\begin{aligned} &\boldsymbol{\phi}_k^{m(\tau)}(x_1 - x_1', x_2 - x_2', x_3) = \boldsymbol{R}(\theta) \boldsymbol{H}_k^{m(\tau)}(r, \theta) \boldsymbol{\Psi}_k(x_3) \quad (\tau = 1.2) \\ &\boldsymbol{S}_k^m(x_3') = \boldsymbol{\Psi}_k(x_3')^{\mathrm{T}} \hat{\boldsymbol{s}}_k^m \boldsymbol{R}(0)^{\mathrm{T}} \end{aligned} \tag{54}$$

Note that r and θ in Eq. (54) are

$$r = \sqrt{(x_1 - x_1')^2 + (x_2 - x_2')^2} \tag{55}$$

$$\theta = \tan^{-1} \frac{x_2 - x_2'}{x_1 - x_1'} \tag{56}$$

Derivation of the Green's function for traction is almost the same. The result, which is based on $\boldsymbol{T}_\beta$, is

$$\begin{aligned} \boldsymbol{T}(\boldsymbol{r}, \boldsymbol{r}') = &-\frac{\mathrm{i}}{4} \sum_{m=-2}^{2} \sum_{k \in \sigma_{\mathrm{p}}} s(k) k \boldsymbol{\phi}_k^{m(\tau)}(x_1 - x_1', x_1 - x_2', x_3) \boldsymbol{E}_k^{-1} \boldsymbol{D}_k^m(x_3') \\ &-\frac{\mathrm{i}}{4} \sum_{m=-2}^{2} \int_{\sigma_{\mathrm{c}}} k \boldsymbol{\phi}_k^{m(2)}(x_1 - x_1', x_1 - x_2', x_3) \boldsymbol{E}_k^{-1} \boldsymbol{D}_k^m(x_3') |\mathrm{d}k| \end{aligned} \tag{57}$$

where $\boldsymbol{T}(\boldsymbol{r}, \boldsymbol{r}')$ is the Green's function for traction and the components of $\boldsymbol{D}_k^m$ are obtained from

$$[\boldsymbol{D}_k^m(x_3')]_{\alpha\beta} = \lambda n_\beta [\boldsymbol{S}_{\gamma k}^m(x_3')]_{\alpha\gamma} + \mu n_\gamma [\boldsymbol{S}_{\gamma k}^m(x_3')]_{\alpha\beta} + \mu n_\gamma [\boldsymbol{S}_{\beta k}^m(x_3')]_{\alpha\gamma} \tag{58}$$

where $[\ ]_{\alpha\beta}$ denotes the components of the matrix, n describes the normal vector used to define the traction and the summation convention is applied to Eq. (58). In addition,

$$\begin{aligned} &\boldsymbol{S}_{\beta k}^m = \boldsymbol{\Psi}_k(x_3')^{\mathrm{T}} \hat{\boldsymbol{d}}_{\beta k}^m \boldsymbol{R}(0)^{\mathrm{T}} \quad (\beta = 1, 2) \\ &\boldsymbol{S}_{\beta k}^m = \boldsymbol{\Psi}_k'(x_3')^{\mathrm{T}} \hat{\boldsymbol{s}}_k^m \boldsymbol{R}(0)^{\mathrm{T}} \quad (\beta = 3) \end{aligned} \tag{59}$$

where $\boldsymbol{\Psi}_k'(x_3')$ is the derivative of the eigenfunction.

4. Integral equation method for the scattering problem

Let us consider the scattering problem, the concept of which is shown in Fig. 1. The displacement field outside the scattering object can be decomposed into the following form:

$$\boldsymbol{u} = \boldsymbol{u}_{\mathrm{F}} + \boldsymbol{u}_{\mathrm{S}} \tag{60}$$

where $\boldsymbol{u}_{\mathrm{F}}$ is the free field response of the layered medium due to a plane incident wave and $\boldsymbol{u}_{\mathrm{S}}$ is the scattering wave radiating from the scattering object. In the first part of this section, a brief overview for the

free field response is presented. After that, a boundary integral equation for the scattering problem is discussed.

To obtain the free field response, let the displacement field be expressed by the three scalar potentials as shown in Appendix A,

$$\boldsymbol{u}_{\mathrm{F}} = \nabla\varphi + \nabla \times \nabla \times (\psi \boldsymbol{e}_z) + \nabla \times (\chi \boldsymbol{e}_z) \tag{61}$$

The scalar potentials for the plane wave are in the forms of

$$\begin{aligned} \varphi(\boldsymbol{r}) &= \exp(-\mathrm{i}(k_1 x_1 + k_2 x_2))\hat{\varphi}_k(x_3) \\ \psi(\boldsymbol{r}) &= \exp(-\mathrm{i}(k_1 x_1 + k_2 x_2))\hat{\psi}_k(x_3) \\ \chi(\boldsymbol{r}) &= \exp(-\mathrm{i}(k_1 x_1 + k_2 x_2))\hat{\chi}_k(x_3) \end{aligned} \tag{62}$$

where $\hat{\varphi}_k$, $\hat{\psi}_k$ and $\hat{\chi}_k$ satisfy the following:

$$\begin{aligned} (\partial_3^2 + k_L^2 - k^2)\hat{\varphi}_k(x_3) &= 0 \\ (\partial_3^2 + k_T^2 - k^2)\hat{\psi}_k(x_3) &= 0 \\ (\partial_3^2 + k_T^2 - k^2)\hat{\chi}_k(x_3) &= 0 \end{aligned} \tag{63}$$

where $k^2 = k_1^2 + k_2^2$. Substitution of Eq. (62) into Eq. (61) leads to the following:

$$\begin{pmatrix} u_{\mathrm{F}1}(x_1, x_2, x_3) \\ u_{\mathrm{F}2}(x_1, x_2, x_3) \\ u_{\mathrm{F}3}(x_1, x_2, x_3) \end{pmatrix} = \begin{bmatrix} \frac{1}{k}\partial_1 h_k(x_1, x_2) & \frac{1}{k}\partial_2 h_k(x_1, x_2) & 0 \\ \frac{1}{k}\partial_2 h_k(x_1, x_2) & -\frac{1}{k}\partial_1 h_k(x_1, x_2) & 0 \\ 0 & 0 & h_k(x_1, x_2) \end{bmatrix} \begin{pmatrix} \hat{\boldsymbol{u}}_{kxy}(z) \\ \hat{u}_{k\mathrm{SH}}(z) \\ \hat{u}_{kz}(z) \end{pmatrix} \tag{64}$$

where $u_{\mathrm{F}j}$ $(j = 1, 2, 3)$ is the component of $\boldsymbol{u}_{\mathrm{F}}$ and

$$h_k(x_1, x_2) = \exp(-\mathrm{i}(k_1 x_1 + k_2 x_2)) \tag{65}$$

Note that $(\hat{\boldsymbol{u}}_{kxy}, \hat{u}_{k\mathrm{SH}}, \hat{u}_{kz})^{\mathrm{T}}$ is the wave function in the wavenumber domain satisfying

$$\mathscr{A}_k \begin{pmatrix} \hat{u}_{kz} \\ \hat{\boldsymbol{u}}_{kxy} \\ \hat{u}_{k\mathrm{SH}} \end{pmatrix} = \boldsymbol{0} \tag{66}$$

The method for composing the solution for Eq. (66) is possible by means of the propagator matrix method shown in Appendix B.

To obtain the boundary integral equation, the definition of the radiation condition for an elastic layered half space is necessary. However, it would be very difficult to present the radiation condition for a generalized elastic layered wave field as in the form of the Sommerfeld radiation condition. Therefore, instead of presenting such conditions, we define the radiation solution of an elastic layered half space in the form:

Definition 1. The radiation solution of an elastic layered half space from a scattering object is the solution expressed by boundary values and the Green's functions such that

$$\boldsymbol{u}(\boldsymbol{r}) = -\int_{\Gamma} \boldsymbol{T}(\boldsymbol{r}, \boldsymbol{r}')\boldsymbol{u}(\boldsymbol{r}')\,\mathrm{d}\Gamma(\boldsymbol{r}') + \int_{\Gamma} \boldsymbol{G}(\boldsymbol{r}, \boldsymbol{r}')\boldsymbol{\tau}(\boldsymbol{r}')\,\mathrm{d}\Gamma(\boldsymbol{r}') \tag{67}$$

where

$$\boldsymbol{r} \in R^2 \times R_+ \setminus (\Gamma \cup \Omega) \tag{68}$$

In addition, we introduce the following assumption:

Assumption 3. The scattering wave shown in Eq. (60) is the radiation solution. Namely,

$$\boldsymbol{u}_{\mathrm{S}}(\boldsymbol{r}) = -\int_{\Gamma} \boldsymbol{T}(\boldsymbol{r},\boldsymbol{r}')\boldsymbol{u}_{\mathrm{S}}(\boldsymbol{r}')\,\mathrm{d}\Gamma(\boldsymbol{r}') + \int_{\Gamma} \boldsymbol{G}(\boldsymbol{r},\boldsymbol{r}')\boldsymbol{\tau}_{\mathrm{S}}(\boldsymbol{r}')\,\mathrm{d}\Gamma(\boldsymbol{r}') \tag{69}$$

Let us investigate one property of the definition of the radiation solution. Assume that $\boldsymbol{L}$ be the operator for the elastic wave propagation. Namely,

$$\boldsymbol{L} = (\lambda+\mu)\nabla\nabla\cdot + \mu\nabla^2 + \rho\omega^2$$

The definition of the Green's function is

$$\boldsymbol{L}\boldsymbol{U}(\boldsymbol{r},\boldsymbol{r}') = -\mathbf{1}\delta(\boldsymbol{r}-\boldsymbol{r}') \tag{70}$$

Reciprocity of the Green's function

$$\boldsymbol{U}(\boldsymbol{r},\boldsymbol{r}') = \boldsymbol{U}(\boldsymbol{r}',\boldsymbol{r})^{\mathrm{T}} \tag{71}$$

ensures the following:

$$\boldsymbol{L}\boldsymbol{U}(\boldsymbol{r}',\boldsymbol{r})^{\mathrm{T}} = -\mathbf{1}\delta(\boldsymbol{r}-\boldsymbol{r}') \tag{72}$$

The reciprocity of the Green function, which can be captured from its eigenfunction expansion form with the symmetry of the energy integrals, describes the property of the exchange of the source and field points. At this point, let B be the intersection of a large sphere including the scattering object and the layered wave field and Γ_{B} be its boundary. It is possible to derive the following Green's identity for the operator $\boldsymbol{L}$ by integration by parts:

$$\int_{\Omega^*} [\boldsymbol{u}^*(\boldsymbol{r})^{\mathrm{T}}\boldsymbol{L}\boldsymbol{u}(\boldsymbol{r}) - [\boldsymbol{L}\boldsymbol{u}^*(\boldsymbol{r})]^{\mathrm{T}}\boldsymbol{u}(\boldsymbol{r})]\,\mathrm{d}\Omega^*(\boldsymbol{r}) = \int_{\Gamma+\Gamma_{\mathrm{B}}} [\boldsymbol{u}^*(\boldsymbol{r})^{\mathrm{T}}\boldsymbol{\tau}(\boldsymbol{r}) - \boldsymbol{\tau}^*(\boldsymbol{r})^{\mathrm{T}}\boldsymbol{u}(\boldsymbol{r})]\,\mathrm{d}\Gamma(\boldsymbol{r}) \tag{73}$$

where $\boldsymbol{u}$ and $\boldsymbol{u}^*$ are displacement fields, $\boldsymbol{\tau}$ and $\boldsymbol{\tau}^*$ are the corresponding traction vectors and

$$\Omega^* = B \setminus (\Omega \cup \Gamma) \tag{74}$$

Note that the direction of the normal vector at the boundary to define the traction is outward with respect to Ω^*. Now, let

$$\boldsymbol{u}^*(\boldsymbol{r}) = \boldsymbol{U}(\boldsymbol{r}',\boldsymbol{r})^{\mathrm{T}} \tag{75}$$

and

$$\boldsymbol{L}\boldsymbol{u}(\boldsymbol{r}) = \mathbf{0} \tag{76}$$

Then, the following integral equation is derived from Eq. (72) in the case $\boldsymbol{r}' \in \Omega^*$:

$$\boldsymbol{u}(\boldsymbol{r}') = -\int_{\Gamma+\Gamma_{\mathrm{B}}} \boldsymbol{T}(\boldsymbol{r}',\boldsymbol{r})\boldsymbol{u}(\boldsymbol{r})\,\mathrm{d}\Gamma(\boldsymbol{r}) + \int_{\Gamma+\Gamma_{\mathrm{B}}} \boldsymbol{U}(\boldsymbol{r}',\boldsymbol{r})\boldsymbol{\tau}(\boldsymbol{r})\,\mathrm{d}\Gamma(\boldsymbol{r}) \tag{77}$$

Assume that $\boldsymbol{u}$ in Eq. (77) be the radiation solution. Then, the definition of the radiation solution requires

$$\int_{\Gamma_{\mathrm{B}}} \boldsymbol{T}(\boldsymbol{r},\boldsymbol{r}')\boldsymbol{u}(\boldsymbol{r})\,\mathrm{d}\Gamma(\boldsymbol{r}') - \int_{\Gamma_{\mathrm{B}}} \boldsymbol{U}(\boldsymbol{r},\boldsymbol{r}')\boldsymbol{\tau}(\boldsymbol{r}')\,\mathrm{d}\Gamma(\boldsymbol{r}') \to 0 \quad (a \to \infty) \tag{78}$$

for the case of $\boldsymbol{r} \in \Omega^*$, where a denotes the radius of the sphere.

For the free field response, the Green's identity is applied to the region of the scattering object Ω,

$$\int_{\Omega} [\boldsymbol{u}^*(\boldsymbol{r})^{\mathrm{T}}\boldsymbol{L}\boldsymbol{u}(\boldsymbol{r}) - [\boldsymbol{L}\boldsymbol{u}^*(\boldsymbol{r})]^{\mathrm{T}}\boldsymbol{u}(\boldsymbol{r})]\,\mathrm{d}\Omega(\boldsymbol{r}) = \int_{\Gamma} [\boldsymbol{u}^*(\boldsymbol{r})^{\mathrm{T}}\boldsymbol{\tau}(\boldsymbol{r}) - \boldsymbol{\tau}^*(\boldsymbol{r})^{\mathrm{T}}\boldsymbol{u}(\boldsymbol{r})]\,\mathrm{d}\Gamma(\boldsymbol{r}) \tag{79}$$

and the following integral equation is established:

$$-\int_{\Gamma} \boldsymbol{T}(\boldsymbol{r},\boldsymbol{r}')\boldsymbol{u}_{\mathrm{F}}(\boldsymbol{r}')\,\mathrm{d}\Gamma(\boldsymbol{r}')+\int_{\Gamma} \boldsymbol{G}(\boldsymbol{r},\boldsymbol{r}')\boldsymbol{\tau}_{\mathrm{F}}(\boldsymbol{r}')\,\mathrm{d}\Gamma(\boldsymbol{r}')=\boldsymbol{0} \tag{80}$$

where $\boldsymbol{r}\in R^2\times R_+\setminus(\Omega\cup\Gamma)$. Addition of Eqs. (69) and (80) leads to the following:

$$\boldsymbol{u}(\boldsymbol{r})+\int_{\Gamma} \boldsymbol{T}(\boldsymbol{r},\boldsymbol{r}')\boldsymbol{u}(\boldsymbol{r}')\,\mathrm{d}\Gamma(\boldsymbol{r}')=\int_{\Gamma} \boldsymbol{U}(\boldsymbol{r},\boldsymbol{r}')\boldsymbol{\tau}(\boldsymbol{r}')\,\mathrm{d}\Gamma(\boldsymbol{r}')+\boldsymbol{u}_{\mathrm{F}}(\boldsymbol{r}),\quad \boldsymbol{r}\in R^2\times R_+\setminus(\Omega\cup\Gamma) \tag{81}$$

At this point, let $\boldsymbol{r}$ approach the boundary of the scattering object. Then, the following boundary integral equation is established:

$$\boldsymbol{c}\boldsymbol{u}(\boldsymbol{r})+\int_{\Gamma} \boldsymbol{T}(\boldsymbol{r},\boldsymbol{r}')\boldsymbol{u}(\boldsymbol{r}')\,\mathrm{d}\Gamma(\boldsymbol{r}')=\int_{\Gamma} \boldsymbol{U}(\boldsymbol{r},\boldsymbol{r}')\boldsymbol{\tau}(\boldsymbol{r}')\,\mathrm{d}\Gamma(\boldsymbol{r}')+\boldsymbol{u}_{\mathrm{F}}(\boldsymbol{r})\quad(\boldsymbol{r}\in\Gamma) \tag{82}$$

where $\boldsymbol{c}$ is the coefficient matrix of the free term of the boundary integral equation.

For the inclusion of the scattering object, the boundary integral equation is as follows:

$$\boldsymbol{c}^{(i)}(\boldsymbol{r})\boldsymbol{u}^{(i)}(\boldsymbol{r})+\int_{\Gamma} \boldsymbol{T}^{(i)}(\boldsymbol{r},\boldsymbol{r}')\boldsymbol{u}^{(i)}(\boldsymbol{r}')\,\mathrm{d}\Gamma(\boldsymbol{r}')=\int_{\Gamma} \boldsymbol{U}^{(i)}(\boldsymbol{r},\boldsymbol{r}')\boldsymbol{\tau}^{(i)}(\boldsymbol{r}')\,\mathrm{d}\Gamma(\boldsymbol{r}')\quad(\boldsymbol{r}\in\Gamma) \tag{83}$$

where the superscript (i) denotes the variable related to the inclusion of the scattering object. In addition, the direction of the normal vector to define the traction vector $\boldsymbol{\tau}^{(i)}$ is away from the scattering object. According to standard texts on the boundary element method (for example, Brebbia and Walker, 1980), the components of the Green's functions for inclusion can be written as follows:

$$U^{(i)}_{\alpha\beta}(\boldsymbol{r},\boldsymbol{r}')=\frac{\delta_{\alpha\beta}}{4\pi\mu^{(i)}}\left(\Phi^{(T)}_1(r)+\Phi^{(T)}_2(r)-(c^{(i)}_T/c^{(i)}_L)^2\Phi^{(L)}_2(r)\right)+\frac{1}{4\pi\mu^{(i)}}\frac{\partial r}{\partial x'_\alpha}\frac{\partial r}{\partial x'_\beta}\left(-\Phi^{(T)}_3(r)+(c^{(i)}_T/c^{(i)}_L)^2\Phi^{(L)}_2(r)\right) \tag{84}$$

where r is the distance between the field and source points, $c^{(i)}_T$ and $c^{(i)}_L$ are the S and P wave velocities, respectively and $\Phi^{(p)}_j$ $(j=1,2,3,\ p=T,L)$ is the wavefunction given by

$$\begin{aligned}
\Phi^{(p)}_1(r)&=\frac{\exp(-\mathrm{i}k^{(i)}_{\mathrm{p}}r)}{r}\\
\Phi^{(p)}_2(r)&=-\left(\frac{1}{k^{(i)2}_{\mathrm{p}}r^2}+\frac{i}{k^{(i)}_{\mathrm{p}}r}\right)\frac{\exp(-\mathrm{i}k^{(i)}_{\mathrm{p}}r)}{r}\\
\Phi^{(p)}_3(r)&=\Phi^{(p)}_1(r)+3\Phi^{(p)}_2(r)\quad(p=T,L)
\end{aligned} \tag{85}$$

where $k^{(i)}_T$ and $k^{(i)}_L$ are the wavenumbers for the S and P waves for the inclusion, respectively. The Green's function for the traction is obtained from the following identity:

$$T^{(i)}_{\alpha\beta}(\boldsymbol{r},\boldsymbol{r}')=\left(\lambda^{(i)}\delta_{\beta\gamma}\frac{\partial U^{(i)}_{\alpha\eta}}{\partial x'_\eta}+\mu^{(i)}\left(\frac{\partial U^{(i)}_{\alpha\gamma}}{\partial x'_\beta}+\frac{\partial U^{(i)}_{\alpha\beta}}{\partial x'_\gamma}\right)\right)n_\gamma \tag{86}$$

It is a simple process to couple the boundary integral equations (82) and (83) by means of Eq. (7). As a result, the scattering wave field can be analyzed.

Once the boundary values are obtained by boundary element analysis, the scattering waves are determined by means of Eq. (82):

$$\boldsymbol{u}_{\mathrm{S}}(\boldsymbol{r})=-\int_{\Gamma} \boldsymbol{T}(\boldsymbol{r},\boldsymbol{r}')\boldsymbol{u}(\boldsymbol{r}')\,\mathrm{d}\Gamma(\boldsymbol{r}')+\int_{\Gamma} \boldsymbol{U}(\boldsymbol{r},\boldsymbol{r}')\boldsymbol{\tau}(\boldsymbol{r}')\,\mathrm{d}\Gamma(\boldsymbol{r}') \tag{87}$$

Substituting Eqs. (53) and (57) into (87) and performing the boundary integration leads to the following representation of scattering waves:

$$\boldsymbol{u}_{\mathrm{s}}(\boldsymbol{r}) = \sum_{k\in\sigma_{\mathrm{p}}} \boldsymbol{y}_k(\boldsymbol{r}) + \int_{\sigma_{\mathrm{c}}} \boldsymbol{y}_k(\boldsymbol{r})\,|\mathrm{d}k| \tag{88}$$

where $\boldsymbol{y}_k$ is denoted by

$$\begin{aligned}\boldsymbol{y}_k(\boldsymbol{r}) = {} & \frac{\mathrm{i}}{4}\sum_{m=-2}^{2} s(k)\int_{\Gamma} k\boldsymbol{\phi}_k^{m(\tau)}(x_1-x_1',x_1-x_2',x_3)\boldsymbol{E}_k^{-1}\boldsymbol{D}_k^{m}(x_3')\boldsymbol{u}(\boldsymbol{r}')\,\mathrm{d}\Gamma(\boldsymbol{r}') \\ & -\frac{\mathrm{i}}{4}\sum_{m=-1}^{+1} s(k)\int_{\Gamma} k\boldsymbol{\phi}_k^{m(\tau)}(x_1-x_1',x_1-x_2',x_3)\boldsymbol{E}_k^{-1}\boldsymbol{S}_k^{m}(x_3')\boldsymbol{\tau}(\boldsymbol{r}')\,\mathrm{d}\Gamma(\boldsymbol{r}')\end{aligned} \tag{89}$$

Eq. (88) shows that the scattering waves are decomposed into wavefunctions on the spectra. As shown in the following examples, the decomposition of the scattering waves will aid in the understanding of their properties.

5. Numerical examples

A computer program based on the formulation presented here was developed for the analysis of numerical examples. The propagator matrix method was employed in the program to obtain the eigenfunctions that constitute the Green's functions for a multi-layered medium. The examples shown below are for the verification of the developed program as well as to investigate radiation of the scattering waves from an object in a layered medium.

Fig. 6 shows the analyzed model, in which a spheroidal scattering object is embedded in a two-layered elastic half space and a plane incident SV wave is considered. The amplitude of the incident wave is normalized such that the free field response in the wavenumber domain due to the incident wave satisfies

$$|\hat{\boldsymbol{u}}_{kxy}|^2 + |\hat{\boldsymbol{u}}_{kz}|^2 = 1 \quad [\mathrm{cm}^2] \tag{90}$$

at the free boundary, where $\hat{\boldsymbol{u}}_{kxy}$ and $\hat{\boldsymbol{u}}_{kz}$ are shown in Eq. (64). The normalization means that the unit of the displacements shown below is [cm].

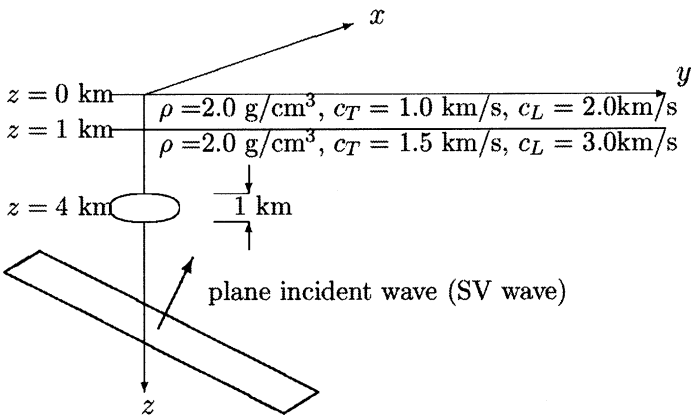

Fig. 6. Analyzed model for the scattering problem. The scattering object is in a two-layered elastic half space.

As shown in the analyzed model, a cartesian coordinate system is employed in this section. The frequency of the analysis is 1.0 Hz, and the direction vector of the plane incident SV wave is

$$\boldsymbol{a} = (1, 1, -1) \tag{91}$$

in terms of the coordinate system shown in Fig. 6. The mass density of the layered medium is 2.0 $\mathrm{g\,cm^{-3}}$ both for the surface layer and the half space. The S and P wave velocities for the surface layer are 1.0 and 2.0 $\mathrm{km\,s^{-1}}$, respectively, while those for the half space are 1.5 and 3.0 $\mathrm{km\,s^{-1}}$, respectively. The depth of the surface layer is 1.0 km. The boundary elements for the spheroidal object are shown in Fig. 7.

Fig. 8 shows the location of the wavenumbers for the complex Rayleigh wave modes in the first quadrant of the complex wavenumber plane for the analyzed model at a frequency of 1.0 Hz. The wavenumbers are obtained from the following Newton–Raphson scheme:

$$k_{j+1} = k_j - \frac{F(k_j)}{F'(k_j)} \quad (j = 1, 2, \ldots) \tag{92}$$

$$F'(k_j) = \frac{1}{2\pi \mathrm{i}} \oint \frac{F(k)}{(k - k_j)^2}\, \mathrm{d}k \tag{93}$$

where k_j is an approximate wavenumber for the complex Rayleigh wave mode and $F(k)$ is the characteristic function for the wave field. The contour integral for Eq. (93) is performed for the small circle around k_j. As can be seen in Fig. 8, the complex Rayleigh wave modes distribute almost linearly in the semi-logarithmic graph of the complex wavenumber plane. The complex Rayleigh wave modes are shown to approximate 1500 $\mathrm{km^{-1}}$ at their absolute values. These high absolute values are required for the calculation of the Green's functions for cases in which the horizontal range of the field and source points are very small, namely the horizontal range is approximately 0.02 km.

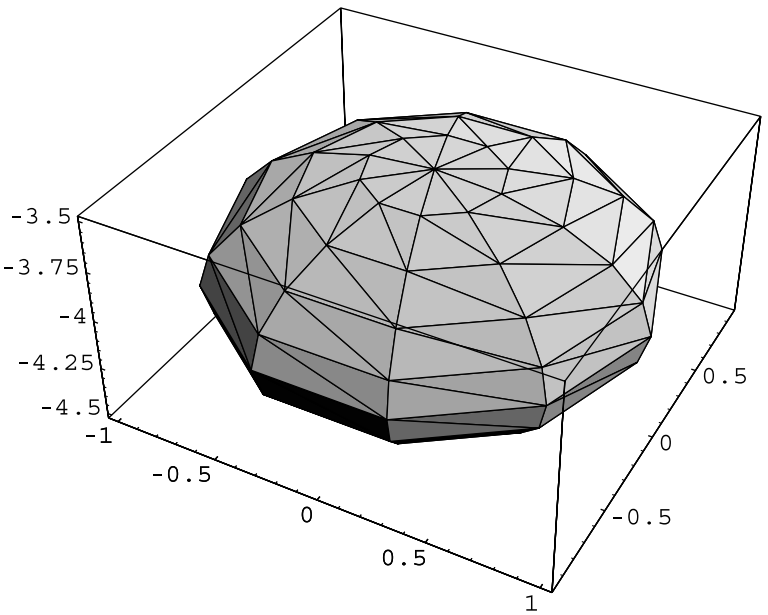

Fig. 7. Boundary elements for the scattering object.

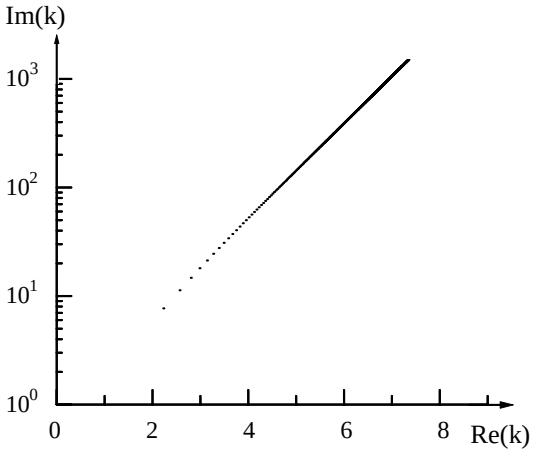

Fig. 8. Location of the wavenumbers for the complex Rayleigh wave modes in the first quadrant of the complex wavenumber plane.

First, let the properties for the inclusion of the scattering object be identical to those of the surrounding, so that the present solution for the wave field becomes a free field response, which can be calculated using the propagator matrix method. Figs. 9 and 10 show comparisons of the displacements of the free field responses and the present solutions along the y-axis on the free surface. According to the figures, the results show almost complete agreement, which validates the accuracy of the proposed method. Therefore, the complete eigenfunction expansion form of the Green's functions for displacement and traction are applicable to the boundary element analysis.

Next, let the inclusion of the object be softer. Here, the S and P wave velocities for inclusion are 0.75 and 1.5 $\mathrm{km\,s^{-1}}$, respectively, and the mass density is 2.0 $\mathrm{g\,cm^{-3}}$. Fig. 11 shows the distribution of the displacements of the wave field at the free surface. In addition, Figs. 12 and 13 show the free field response and propagation of the scattering wave at the free surface, respectively. Note that the result in Fig. 11 is the sum of the results in Figs. 12 and 13. In other words, the differences between Figs. 11 and 12 are due to the effects of the scattering wave. The arrow shown in the figures is the projection of the direction of the incident wave onto the x–y plane.

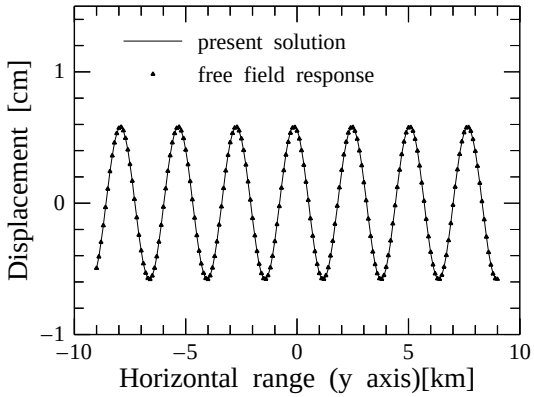

Fig. 9. Comparison of displacements in x-direction at the surface along y-coordinate.

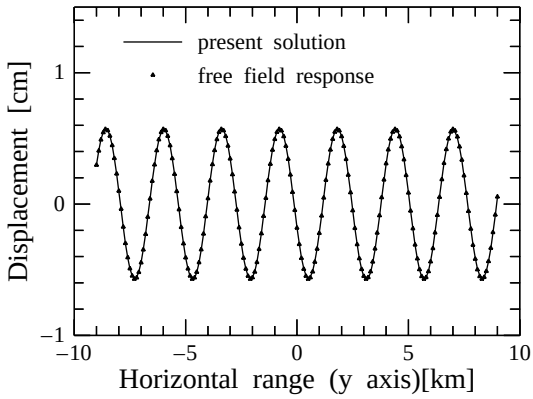

Fig. 10. Comparison of displacements in z-direction at the surface along y-coordinate.

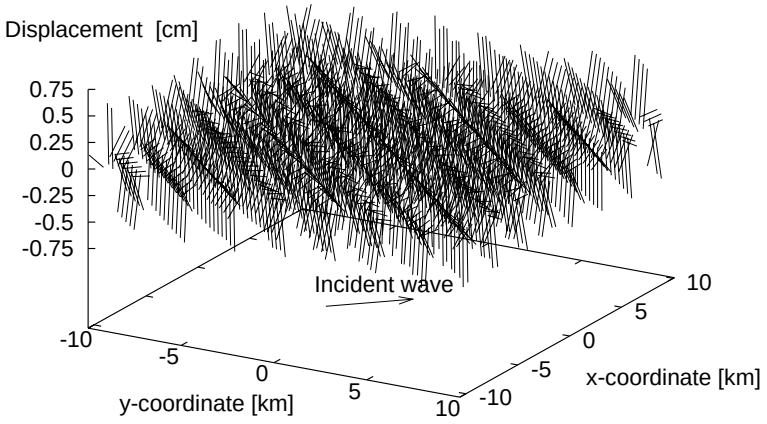

Fig. 11. Total scattering wave field at the free surface.

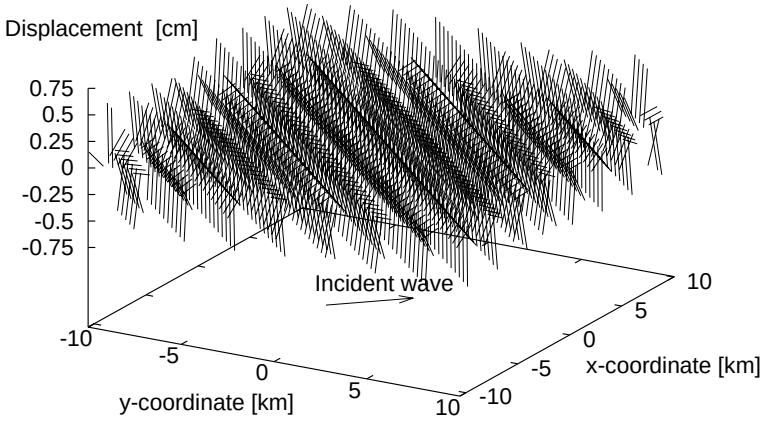

Fig. 12. Free field response at the free surface.

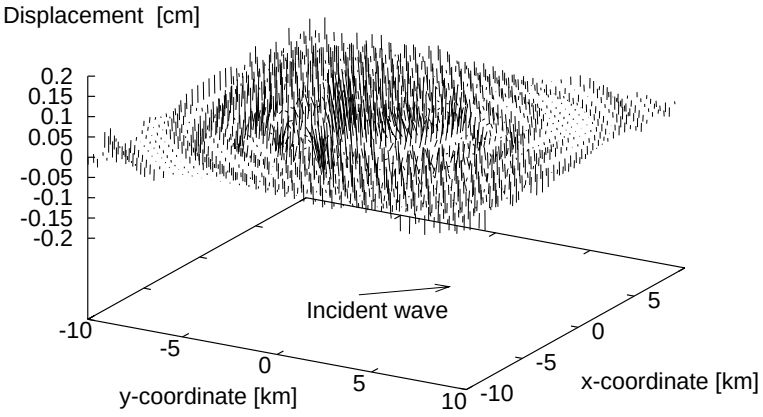

Fig. 13. Radiation of the scattering wave at the free surface.

As shown in Fig. 11, the effects of the scattering wave can be seen mostly above the scattering object. In the range of the far field of the object, the present solution and the free field response tend to agree. According to Fig. 13, the scattering waves propagate approximately isotropically around the scattering object. Furthermore, the amplitudes of the displacement in the backward side of the scattering object are larger than those in the forward side. The wavelengths of the scattering wave are shorter on the backward side of the object than those on the forward side. Relatively large amplitudes for the vertical displacement can be found in the immediate vicinity of the scattering object.

At this point, let us investigate the properties of the scattering wave in terms of the modes for the discrete and continuous spectra. Here, the scattering waves are decomposed into the modes based on Eq. (89). Note that the wavenumber for the fundamental Rayleigh wave mode is 6.69 km^{-1} and that for the first higher mode is 4.68 km^{-1}. In addition, the wavenumber for the fundamental Love wave mode is 6.12 km^{-1} and that for the first higher mode is 4.79 km^{-1} at a frequency of 1.0 Hz. The wavenumber of the S wave in the half space is 4.19 km^{-1}.

Fig. 14 is the propagation of the fundamental Rayleigh wave mode decomposed from the scattering waves. As can be seen in Fig. 14, the fundamental Rayleigh wave mode clearly propagates in the forward direction. For the lateral side of the scattering object, the amplitudes of the mode are very small. The displacement amplitudes in the backward side of the object are relatively large, while the wave forms in this area are not clear when compared with the propagation of the mode in the forward direction.

Fig. 15 shows the distribution of the amplitudes of the complex Rayleigh wave mode for $k = (1.33 + 3.41\mathrm{i})\ km^{-1}$. As shown in the figure, relatively large displacement amplitudes can be seen in the immediate vicinity of the scattering object, and the amplitudes reduce rapidly towards the far field. The distribution of displacement exhibits directionality. Namely, the displacements can be seen in the forward and backward side of the scattering object. Here, displacements in the vertical direction are outstanding.

Fig. 16 shows the propagation of the fundamental Love wave mode decomposed from the scattering waves. The propagation shows a rotational motion around the object. In addition, the displacement amplitudes are found to be very small. The reason for the very small displacement amplitudes is that the Love wave is caused by SH waves which are not included in the free field response. The free field response here is constituted by the P and SV waves.

Fig. 17 shows the propagation of the mode for the continuous spectrum. The wavenumber for the mode is 4.19 km^{-1}. This is the wavenumber of the S wave for the half space. According to Fig. 17, the scattering waves propagate in the forward and backward direction with relatively larger displacement amplitudes

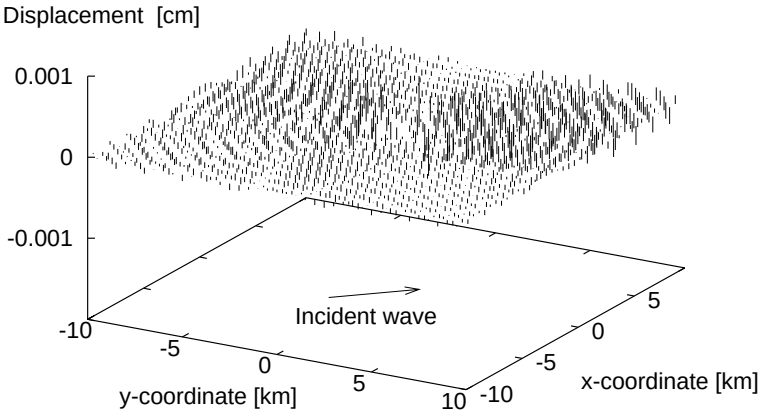

Fig. 14. Radiation of the fundamental Rayleigh wave mode decomposed from the scattering wave.

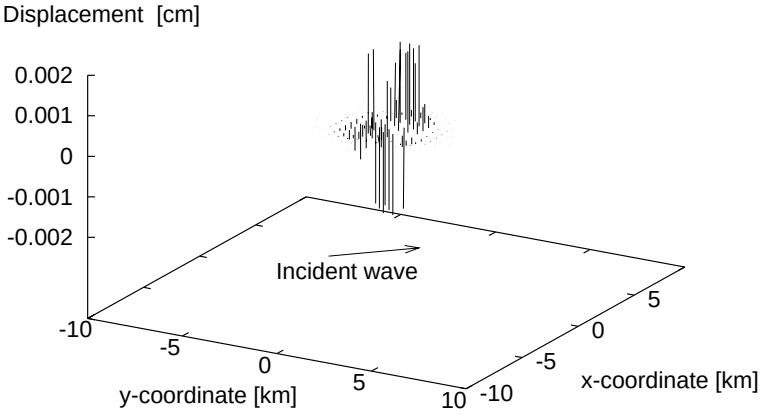

Fig. 15. Distribution of displacements of a complex Rayleigh wave mode decomposed from the scattering wave. The wavenumber for the mode is $k = (1.33 + 3.41\mathrm{i})\ \mathrm{km}^{-1}$.

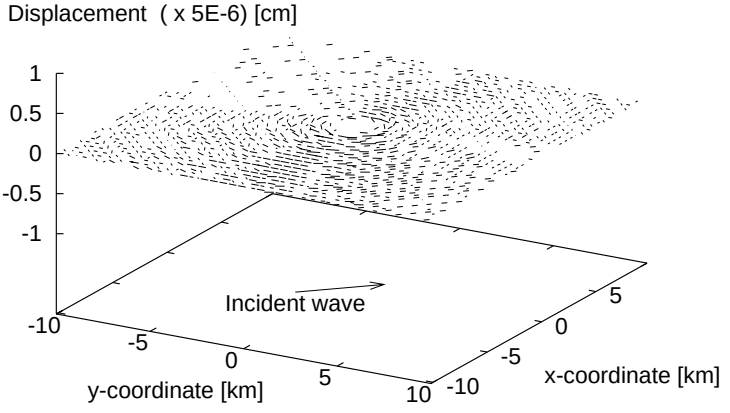

Fig. 16. Radiation of the fundamental Love wave mode decomposed from the scattering wave.

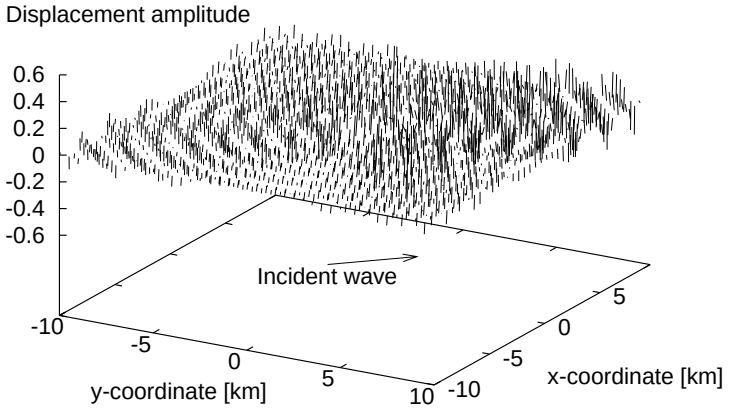

Fig. 17. Radiation of the scattering wave for the continuous spectrum. The wavenumber is $k = 4.19$ km^{-1}.

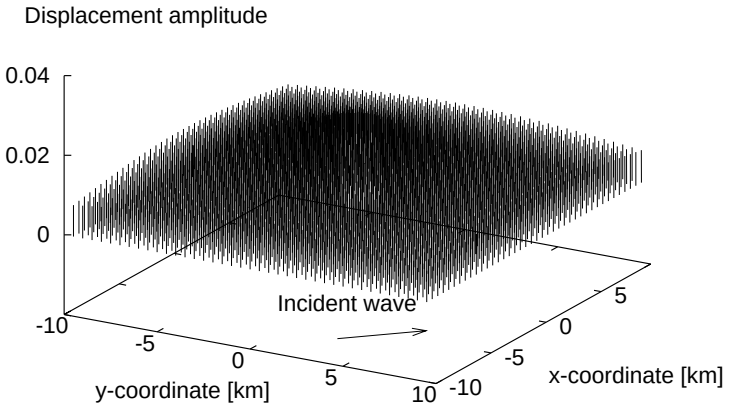

Fig. 18. Radiation of the scattering wave for the continuous spectrum. The wavenumber is $k = 0.0$ km^{-1}.

compared to those in the lateral side direction. The direction of the displacement is found to be mostly vertical. In addition, the scattering wave spreading to the forward side of the object covers a wider area compared to that spreading to the backward side. Fig. 18 shows the propagation of the mode for the continuous spectrum for $k = 0.0$ km^{-1}. It can be seen that the displacement amplitudes distribute isotropically around the scattering object. The direction of the displacement is also prominent in the vertical direction. The amplitudes decrease monotonously with respect to distance from the object.

According to the properties of the propagation of the modes, the Rayleigh wave mode is found to have directionality during its propagation, while the modes for the continuous spectrum do not have strong directionality. Therefore, the continuous spectrum is more significant in the propagation of the scattering wave shown in Fig. 13.

Fig. 19 shows the spectral amplitude of the scattering wave at a field point of $x = 5$ km, $y = 5$ km at the free surface. Here, the absolute values of $\boldsymbol{y}_k$ shown in Eq. (89) are plotted. The vertical lines in the figure denote the amplitude of the normal modes, while the continuous line denotes the amplitude for the continuous spectrum. Note that the negative region of the horizontal axis in the figure denotes the pure imaginary negative wavenumber. The unit of the spectral amplitude for the discrete spectrum is [cm] and

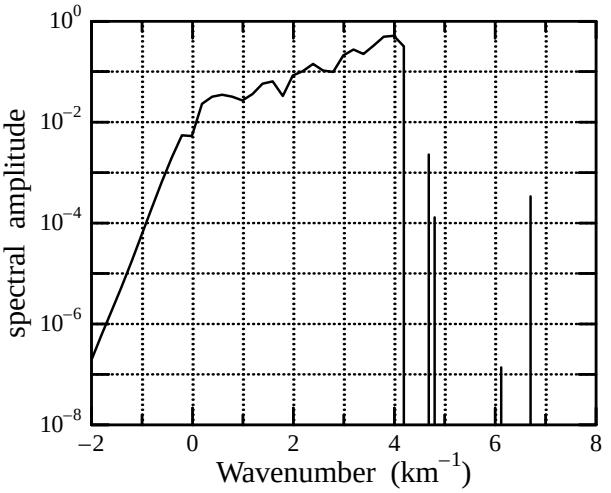

Fig. 19. Spectral structure of the scattering wave at the free surface of $x = 5$ km and $y = 5$ km. The units of the spectral amplitude for the discrete spectrum are [cm] and that for the continuous spectrum are [cm km].

that for the continuous spectrum is [cm km]. It is found from Fig. 19 that the amplitudes of the higher modes for the discrete spectrum are larger than those of the lower modes. The reason for this is that the wavenumber for the plane incident wave is in the continuous spectrum, which is closer to the higher modes for the discrete spectrum. As for the spectral amplitude of the continuous spectrum, the amplitude is higher in the positive real wavenumber range than that in the negative pure imaginary wavenumber range. The reason for this is that the wavenumber for the plane incident wave is in the continuous spectrum for the positive real wavenumber and the horizontal wavefunction decreases rapidly in the pure imaginary negative wavenumber range due to the properties of the Hankel function.

One of the advantages of the present Green's function is that it simplifies the formulation for the boundary integral equation method. The reason for this is that complicated information for the layered structure can be imposed on the eigenfunctions for the spectra. The present Green's function also enables us to decompose scattering waves into the modes for the spectra, which helps in understanding their properties. Furthermore, accurate values can be calculated by means of the Green's function, even in the case that the field and source points are close to each other and when the points are located in the area far from the free surface. The main disadvantage of the present Green's function is that it requires significant processing time when the horizontal distance between the field and source points are very small. This is due to the slow convergence of the spectral integral. The complex Rayleigh wave modes required by the present Green's function also complicate the usage, since it is an elaborate process to find out and to identify them.

6. Conclusions

A formulation and numerical examples for the analysis of scattering waves caused by interaction between an object and a plane incident wave in an elastic layered half space were presented in this paper. For the analysis, the complete eigenfunction expansion form of the Green's function and the boundary integral equation method were employed. At first, the complete eigenfunction expansion form of the Green's functions due to single and double sources were derived. Based on the Green's functions, the singularity of the horizontal wavefunction for the eigenfunction expansion form of the Green's functions were investigated. The

result clarified that the singularity did not have any effects on the Green's functions. Namely, the Green's functions were simply expressed by the summation and integration of the eigenfunctions for the discrete and continuous spectra. Next, a method for the application of the Green's functions to the boundary integral equation method as well as several numerical results were shown. According to the numerical results, the complete eigenfunction expansion form of the Green's function were applicable to the boundary element analysis. Furthermore, a spectral structure as well as the radiation of the scattering wave obtained from the present method were found to be useful to explain the properties of the scattering waves. For example, the propagation of the fundamental Rayleigh wave mode decomposed from the scattering wave exhibited strong directionality when compared to that for the continuous spectrum. The scattering wave propagated isotropically around the object, so that the components of the continuous spectrum were more significant for the scattering wave than those of the discrete spectrum.

Appendix A. Fourier–Hankel transform for an elastic layered wave field

We investigate here a Fourier–Hankel transform for a vector field of an elastic layered medium. The derivation of the transform is presented formally. In the following, the infinite series for m can be seen, however, it can be reduced into the finite sum in the case that the point source is applied. The problem of the convergence of the wavenumber integral is also discussed in the main text of this article. Following Aki and Richards (1980), three scalar potentials φ, ψ and χ are employed to represent a displacement field for an elastic layered wave medium

$$\boldsymbol{u} = \nabla\varphi + \nabla \times \nabla \times (\psi \boldsymbol{e}_z) + \nabla \times (\chi \boldsymbol{e}_z) \tag{A.1}$$

where $\boldsymbol{e}_z$ is the base vector for the vertical coordinate. Note that φ, ψ and χ are for the P, SV and SH waves, respectively. Let the scalar potentials be expressed in the following form:

$$\begin{aligned}
\varphi(\boldsymbol{r}) &= \frac{1}{2\pi} \sum_{m=-\infty}^{\infty} \exp(\mathrm{i}m\theta) \int_0^{\infty} kJ_m(kr)\hat{\varphi}_k^m(z)\,\mathrm{d}k \\
\psi(\boldsymbol{r}) &= \frac{1}{2\pi} \sum_{m=-\infty}^{\infty} \exp(\mathrm{i}m\theta) \int_0^{\infty} kJ_m(kr)\hat{\psi}_k^m(z)\,\mathrm{d}k \\
\chi(\boldsymbol{r}) &= \frac{1}{2\pi} \sum_{m=-\infty}^{\infty} \exp(\mathrm{i}m\theta) \int_0^{\infty} kJ_m(kr)\hat{\chi}_k^m(z)\,\mathrm{d}k
\end{aligned} \tag{A.2}$$

where m is the circumferential order number, k is the wavenumber and J_m is the first kind of the Bessel function of the order m. Substituting Eq. (A.2) into Eq. (A.1) leads to the following:

$$\boldsymbol{u}(\boldsymbol{r}) = \frac{1}{2\pi} \sum_{m=-\infty}^{\infty} \int_0^{\infty} k\boldsymbol{H}_k^m(r,\theta)\hat{\boldsymbol{u}}_k^m(z)\,\mathrm{d}k \tag{A.3}$$

where $\boldsymbol{H}_k^m$ is called here the horizontal wavefunction with components

$$\boldsymbol{H}_k^m(r,\theta) = \begin{bmatrix} Y_k^m(r,\theta) & 0 & 0 \\ 0 & \frac{1}{k}\partial_r Y_k(r,\theta) & \frac{1}{kr}\partial_\theta Y_k^m(r,\theta) \\ 0 & \frac{1}{kr}\partial_\theta Y_k^m(r,\theta) & -\frac{1}{k}\partial_r Y_k^m(r,\theta) \end{bmatrix} \tag{A.4}$$

where

$$Y_k^m(r,\theta) = J_m(kr)\exp(\mathrm{i}m\theta) \tag{A.5}$$

Note that the superscript m does not denote the power and ∂ is a partial differential operator with respect to the parameter given by the subscript. In addition, the array of the components of $\hat{\boldsymbol{u}}_k^m$ are given by

$$\hat{\boldsymbol{u}}_k^m(z) = \begin{bmatrix} \hat{u}_{zk}^m(z) \\ \hat{u}_{rk}^m(z) \\ \hat{u}_{\theta k}^m(z) \end{bmatrix} \left(= \begin{bmatrix} \partial_z \hat{\varphi}_k^m(z) + k^2 \hat{\psi}_k^m(z) \\ k\hat{\varphi}_k^m(z) + k\partial_z \hat{\psi}_k^m(z) \\ k\hat{\chi}_k^m(z) \end{bmatrix} \right) \tag{A.6}$$

According to Eqs. (A.4) and (A.6), the array of the components of $\boldsymbol{u}$ in Eq. (A.3) becomes as follows:

$$\boldsymbol{u} = (u_z, \quad u_r, \quad u_\theta)^{\mathrm{T}} \tag{A.7}$$

There is a relationship between the components of $\boldsymbol{u}$ and $\hat{\boldsymbol{u}}_k^m$ as follows:

$$\begin{aligned} u_z^m &= \int_0^\infty k J_m(kr) \hat{u}_{zk}^m \, \mathrm{d}k \\ u_r^m - \mathrm{i}u_\theta^m &= \int_0^\infty k J_{m-1}(kr)(\hat{u}_{rk}^m + \mathrm{i}\hat{u}_{\theta k}^m) \, \mathrm{d}k \\ u_\theta^m - \mathrm{i}u_r^m &= \int_0^\infty k J_{m+1}(kr)(\hat{u}_{\theta k}^m + \mathrm{i}\hat{u}_{rk}^m) \, \mathrm{d}k \end{aligned} \tag{A.8}$$

where

$$u_j^m = \int_0^{2\pi} u_j \exp(-\mathrm{i}m\theta) \, \mathrm{d}\theta \quad (j = r, \theta, z) \tag{A.9}$$

Therefore, due to the properties of the Hankel transform, the following equation can be established:

$$\hat{\boldsymbol{u}}_k^m(z) = \int_0^{2\pi} \mathrm{d}\theta \int_0^\infty r \boldsymbol{H}_k^m(r, -\theta) \boldsymbol{u}(\boldsymbol{r}) \, \mathrm{d}r \tag{A.10}$$

In this paper, Eq. (A.10) is used for the Fourier–Hankel transform and Eq. (A.3) for the inverse Fourier–Hankel transform for an elastic transform.

Appendix B. Some properties of the Green's function in the wavenumber domain

This appendix investigates some of the properties of the Green's function in the wavenumber domain together with the asymptotic behaviour in the case that $k \to \infty$. The investigation strongly depends on the propagator matrix method which is used for composing the Green's function in the wavenumber domain. Under these circumstances, a brief explanation of the propagator matrix method is presented. In the following discussion, the layer index l is for the half space.

First of all, consider a layer bounded by $h_j < z < h_{j+1}$ and a homogeneous solution in the layer. The solution for the equation is given by

$$\mathscr{A}_k \hat{\boldsymbol{u}}_k^m(z) = \boldsymbol{0} \quad (h_j < z < h_{j+1}) \tag{B.1}$$

where the differential operator is given by Eq. (16), h_j and h_{j+1} are the vertical coordinates of the layer interfaces and

$$\hat{\boldsymbol{u}}_k^m(z) = (\hat{u}_{zk}^m \quad \hat{u}_{rk}^m \quad \hat{u}_{\theta k}^m)^{\mathrm{T}} \tag{B.2}$$

The local vertical coordinate of the layer ζ_j

$$z = h_j + \zeta_j \quad (0 < \zeta_j < h_{j+1} - h_j) \tag{B.3}$$

is employed to express the solution for Eq. (B.1) such that

$$\begin{aligned}
\hat{u}^m_{zk} &= -\gamma e^{-\gamma_j\zeta_j}\Delta_{1(j)} + \gamma e^{\gamma_j\zeta_j}\Delta_{2(j)} + k^2 e^{-\nu_j\zeta_j}\Delta_{3(j)} + k^2 e^{\nu_j\zeta_j}\Delta_{4(j)} \\
\hat{u}^m_{rk} &= k e^{-\gamma_j\zeta_j}\Delta_{1(j)} + k e^{\gamma_j\zeta_j}\Delta_{2(j)} - \nu_j k e^{-\nu_j\zeta_j}\Delta_{3(j)} - \nu_j k e^{\nu_j\zeta_j}\Delta_{4(j)} \\
\hat{u}^m_{\theta k} &= k e^{-\nu_j\zeta_j}\Delta_{5(j)} + k e^{\nu_j\zeta_j}\Delta_{6(j)}
\end{aligned} \tag{B.4}$$

where $\Delta_{i(j)}$ $(i = 1\text{–}6)$ are the coefficients for the solution for the jth layer and

$$\begin{aligned}
\gamma_j &= \sqrt{k^2 - k^2_{L(j)}} \\
\nu_j &= \sqrt{k^2 - k^2_{T(j)}}
\end{aligned} \tag{B.5}$$

Note that $k_{L(j)}$ and $k_{T(j)}$ are the wavenumbers for the P and S waves in the layer. The components of the traction vector due to displacements $\hat{u}^m_{zk}$, $\hat{u}^m_{rk}$ and $\hat{u}^m_{\theta k}$ are obtained from the following:

$$\begin{pmatrix} \hat{p}^m_{zk} \\ \hat{p}^m_{rk} \\ \hat{p}^m_{\theta k} \end{pmatrix} = \mathscr{P}_k \begin{pmatrix} \hat{u}^m_{rk} \\ \hat{u}^m_{zk} \\ \hat{u}^m_{\theta k} \end{pmatrix} \tag{B.6}$$

where $\mathscr{P}_k$ is the operator defined by

$$\mathscr{P}_k = \begin{bmatrix} (\lambda + 2\mu)\partial_z & -\lambda k & 0 \\ \mu k & \mu\partial_z & 0 \\ 0 & 0 & \mu\partial_z \end{bmatrix} \tag{B.7}$$

Define the states vector and coefficient vector for the layer such that

$$(Y_j(\zeta_j))_j = (\hat{u}^m_{zk}(\zeta_j), \hat{u}^m_{rk}(\zeta_j), \hat{p}^m_{zk}(\zeta_j), \hat{p}^m_{rk}(\zeta_j), \hat{u}^m_{\theta k}(\zeta_j), \hat{p}^m_{\theta k}(\zeta_j))^{\mathrm{T}} \tag{B.8}$$

$$(\Delta)_j = (\Delta_{1(j)}, \Delta_{2(j)}, \Delta_{3(j)}, \Delta_{4(j)}, \Delta_{5(j)}, \Delta_{6(j)})^{\mathrm{T}} \tag{B.9}$$

Then, the states vector $(Y_j(\zeta_j))_j$ can be expressed in the form

$$(Y_j(\zeta_j))_j = [B]_j[\Lambda(\zeta_j)]_j(\Delta)_j \tag{B.10}$$

where the components of the matrix $[B]_j$ and $[\Lambda(\zeta_j)]$ are

$$[B]_j = \begin{bmatrix} -\gamma_j & \gamma_j & k^2 & k^2 & 0 & 0 \\ k & k & -\nu_j k & -\nu_j k & 0 & 0 \\ \mu(k^2+\nu_j^2) & \mu(k^2+\nu_j^2) & -2\mu k^2\nu_j & 2\mu k^2\nu_j & 0 & 0 \\ -2\mu\gamma_j k & 2\mu\gamma_j k & \mu(\nu_j^2+k^2)k & \mu(\nu_j^2+k^2)k & 0 & 0 \\ 0 & 0 & 0 & 0 & k & k \\ 0 & 0 & 0 & 0 & -\mu\nu_j k & \mu\nu_j k \end{bmatrix} \tag{B.11}$$

$$[\Lambda(\zeta_j)]_j = \mathrm{diag}[\exp(-\gamma_j\zeta_j) \quad \exp(\gamma_j\zeta_j) \quad \exp(-\nu_j\zeta_j) \quad \exp(\nu_j\zeta_j) \quad \exp(-\nu_j\zeta_j) \quad \exp(\nu_j\zeta_j)] \tag{B.12}$$

Let the states vector at $\zeta_j = 0$ be denoted by $(Y)_j$ and that at $\zeta_j = h_{j+1} - h_j$ by $(Y)_{j+1}$, where j and $j+1$ are the layer interface number for the upper and lower boundary for the layer. Then, the relationship of the states vectors between $(Y)_j$ and $(Y)_{j+1}$ becomes as follows:

$$(Y)_{j+1} = [T_{j+1,j}](Y)_j \tag{B.13}$$

where $[T_{j+1,j}]$ is the propagator matrix defined by

$$[T_{j+1,j}] = [B]_j[\Lambda(h_{j+1} - h_j)]_j[B]_j^{-1} \tag{B.14}$$

Note that the propagator matrix has the following property:

$$[T_{j+1,j}] = \mathrm{O}\left(\begin{bmatrix} k & k & 1 & 1 & 0 & 0 \\ k & k & 1 & 1 & 0 & 0 \\ k^2 & k^2 & k & k & 0 & 0 \\ k^2 & k^2 & k & k & 0 & 0 \\ 0 & 0 & 0 & 0 & k & k \\ 0 & 0 & 0 & 0 & k^2 & k^2 \end{bmatrix} \exp(k(h_{j+1} - h_j))\right) \quad (k \to \infty) \tag{B.15}$$

where O is the Landau notation and $[T_{j+1,j}]$ is the even function for v_j and γ_j. Therefore, $[T_{j+1,j}]$ does not depend on the branches for v_j and γ_j.

Now, we are in a stage where it is possible to compose the solution for the equation

$$\mathscr{A}_k\hat{\boldsymbol{u}}_k^m(z,z') = -\hat{\boldsymbol{f}}_k^m\delta(z-z') \quad (h_1 < z < \infty) \tag{B.16}$$

where h_1 is the vertical coordinate of the free surface and $\hat{\boldsymbol{f}}_k^m$ is the amplitude of the force vector acting at $z = z'$ whose components are expressed by

$$\hat{\boldsymbol{f}}_k^m = (\hat{f}_{zk}^m \quad \hat{f}_{rk}^m \quad \hat{f}_{\theta k}^m)^{\mathrm{T}} \tag{B.17}$$

The free boundary condition, layer interface conditions and radiation conditions are imposed on Eq. (B.16). The conditions at $z = z'$ due to the source term for $\hat{\boldsymbol{u}}_k^m$ are expressed as

$$\begin{aligned} &\hat{\boldsymbol{u}}_k^m(z'+\epsilon,z') = \hat{\boldsymbol{u}}_k^m(z'-\epsilon,z') \\ &[\mathscr{P}_k\hat{\boldsymbol{u}}_k^m(z,z')]_{z'-\epsilon}^{z'+\epsilon} = -\hat{\boldsymbol{f}}_k^m \end{aligned} \tag{B.18}$$

According to Eq. (B.18) and the layer interface conditions, the relationship between the states vector at the free surface and the coefficient vector for the half space becomes as follows:

$$(\Delta)_l = [B]_l^{-1}[T_{l,l-1}][T_{l-1,l-2}]\cdots[T_{2,1}](Y)_1 - [T_{l,l-1}][T_{l-1,l-2}]\cdots[T_{s+1,s}](Z)_{\mathrm{s}} \tag{B.19}$$

where the subscript 1 for the states vector indicates the free boundary, s and l for those are the layer interface where the force is applied and that between the surface layers and the half space, respectively, and the components of the vector $(Z)_{\mathrm{s}}$ are

$$(Z)_{\mathrm{s}} = \begin{pmatrix} 0 & 0 & \hat{f}_{zk}^m & \hat{f}_{rk}^m & 0 & \hat{f}_{\theta k}^m \end{pmatrix}^{\mathrm{T}} \tag{B.20}$$

In addition, the components of the vectors $(Y)_1$ and $(\Delta)_l$ are as follows due to the free boundary and radiation conditions:

$$\begin{aligned} (Y)_1 &= \begin{pmatrix} \hat{\boldsymbol{u}}_{zk}^m & \hat{\boldsymbol{u}}_{rk}^m & 0 & 0 & \hat{\boldsymbol{u}}_{\theta k}^m & 0 \end{pmatrix}^{\mathrm{T}} \\ (\Delta)_l &= \begin{pmatrix} \Delta_1 & 0 & \Delta_3 & 0 & \Delta_5 & 0 \end{pmatrix}^{\mathrm{T}} \end{aligned} \tag{B.21}$$

The unknown quantities $\hat{\boldsymbol{u}}_{zk}^m$, $\hat{\boldsymbol{u}}_{rk}^m$, $\hat{\boldsymbol{u}}_{\theta k}^m$, Δ_1, Δ_3, Δ_5 are uniquely determined by Eq. (B.19) unless k is in the point spectrum. To show this, express the matrices such that

$$\begin{aligned} [C] &= [B]_l^{-1}[T_{l,l-1}][T_{l-1,l-2}]\cdots[T_{2,1}] \\ [D] &= [B]_l^{-1}[T_{l,l-1}][T_{l-1,l-2}]\cdots[T_{s+1,s}] \end{aligned} \tag{B.22}$$

Then, the solution for Eq. (B.16) at the free surface can be expressed as

$$\hat{\boldsymbol{u}}_k^m(0,z') = \frac{\boldsymbol{M}_k(0,z')}{F(k)}\hat{\boldsymbol{f}}_k^m \tag{B.23}$$

where

$$F(k) = \det\begin{bmatrix} c_{21} & c_{22} & c_{25} \\ c_{41} & c_{42} & c_{45} \\ c_{61} & c_{62} & c_{65} \end{bmatrix} \tag{B.24}$$

$$\boldsymbol{M}_k(0,z') = \begin{bmatrix} c_{21} & c_{22} & c_{25} \\ c_{41} & c_{42} & c_{45} \\ c_{61} & c_{62} & c_{65} \end{bmatrix}^c \begin{bmatrix} d_{23} & d_{24} & d_{26} \\ d_{43} & d_{44} & d_{46} \\ d_{63} & d_{64} & d_{66} \end{bmatrix} \tag{B.25}$$

where c_{ij} and d_{ij} are the components for the matrices $[C]$ and $[D]$ and $[\ ]^c$ denotes the cofactor of the matrix. Based on Eq. (B.23), the solution for an arbitrary depth z can be composed by multiplying a propagator matrix connecting the free boundary and the layer interface boundary at the depth of the field point. As a result, it is possible to give the Green's function in the wavenumber domain in the following form:

$$\boldsymbol{g}_k(z,z') = \frac{\boldsymbol{M}_k(z,z')}{F(k)} \tag{B.26}$$

Note that $F(k)$ is the characteristic function whose roots

$$F(k) = 0 \tag{B.27}$$

constitute the point spectrum for the Green's function in the wavenumber domain.

Now, the asymptotic behaviour of the Green's function in the wavenumber domain in the case that $k \to \infty$ can be evaluated by means of Eq. (B.15) and the procedure for composing the Green's function. It is expressed as follows:

$$\boldsymbol{g}_k(z,z') = \mathrm{O}(k^{-\alpha}\exp(-k|z-z'|)) \quad k \to \infty \tag{B.28}$$

where $\alpha > 0$ is due to multiplications of the propagator matrices.

The procedure for composing the Green's function in the wavenumber domain clarifies that the branch cuts in the complex wavenumber plane are required for γ_l and ν_l. Due to the requirements for the radiation conditions, the permissible sheets for the complex wavenumber plane have to satisfy $\mathrm{Re}(\gamma_l) > 0$ and $\mathrm{Re}(\nu_l) > 0$. Note that the process for composing the Green's function in the wavenumber domain clarifies following property

$$\boldsymbol{g}_{-k}(z,z') = \mathrm{diag}[1 \quad -1 \quad -1]\boldsymbol{g}_k(z,z')\mathrm{diag}[1 \quad -1 \quad -1] \tag{B.29}$$

References

Aki, K., Richards, P.G., 1980. Quantitative Seismology. Freeman and Company, New York, Box. 6.5, pp. 215–216.

Bouchon, M., 1979. Discrete wavenumber representation of elastic wavefields in three space dimensions. J. Geophys. Res. 84, 3609–3614.

Bouchon, M., 1980. Calculation of complete seismograms for an explosive source in layered medium. Geophysics 45, 197–203.

Bouchon, M., 1981. A simple method to calculate Green's functions for elastic layered media. Bull. Seis. Soc. Am. 71, 959–979.

Bouchon, M., 1982. The complete synthesis of seismic crustal phases at regional distances. J. Geophys. Res. 87, 1735–1741.

Bouchon, M., Aki, K., 1977. Discrete wavenumber representation of seismic wave fields. Bull. Seis. Soc. Am. 67, 259–277.

Brebbia, C.A., Walker, S., 1980. Boundary Element Techniques in Engineering. Butterworth and Co. Ltd., London.

Budreck, D.E., Achenbach, J.D., 1989. Three dimensional elastic wave scattering by surface-breaking cracks. J. Acoust. Soc. Am. 86, 395–406.

Colton, D., Kress, R., 1983. Integral Equation Methods in Scattering Theory (Pure and applied mathematics: a Wiley-Interscience series of texts, monographs, and tracts). New York, Wiley.

Colton, D., Kress, R., 1998. Inverse Acoustic and Electromagnetic Scattering Theory. Springer, Berlin.

Fuchs, K., Müller, G., 1971. Computation of synthetic seismograms with the reflectivity method and comparison with observations. Geophysics 23, 417–433.

Haddon, R.A.W., 1984. Computation of synthetic seismograms in layered earth models using leaky modes. Bull. Seis. Soc. Am. 74, 1225–1248.

Haddon, R.A.W., 1986. Exact evaluation of the response of a layered elastic medium to an explosive point source using leaky modes. Bull. Seis. Soc. Am. 76, 1755–1775.

Haddon, R.A.W., 1987. Response of an oceanic wave guide to an explosive point source using leaky modes. Bull. Seis. Soc. Am. 77, 1084–1822.

Harvey, D.J., 1981. Seismogram synthesis using normal mode superposition: the locked mode approximation. Geophys. J. R. Astr. Soc. 66, 37–69.

Kenet, B.L.N., Kerry, N.J., 1979. Seismic waves in a stratified half space. Geophys. J. R. Astr. Soc. 57, 557–583.

Lamb, H., 1904. On the propagation of tremors over the surface of an elastic solid. Phil. Trans. Roy. Soc. Lond. A 203, 1–42.

McLachlan, N.W., 1961. Bessel Functions for Engineers. Oxford University Press, London.

Touhei, T., 2000. A scattering problem by means of the spectral representation of Green's function for a layered acoustic half space. Comput. Mech. 25, 477–488.

Touhei, T., 2002a. Complete eigenfunction expansion form of the Green's function for elastic layered half space. Arch. Appl. Mech. 72, 13–38.

Touhei, T., 2002b. Spectral structures and radiation patterns of the scattering waves in a layered acoustic half space. Arch. Appl. Mech. 72, 363–378.

Watson, T.H., 1972. A real frequency, complex wavenumber analysis of leaking modes. Bull. Seismol. Soc. Am. 62, 369–384.